Microwave Water Level Phase II Analysis

Joseph Park *

*NOAA

National Ocean Service, Center for Operational Products and Services

Water level data from acoustic and microwave ranging sensors covering a period of 19 months at coastal tide stations on both the Atlantic and Pacific coasts are analyzed. Physical mechanisms are identified that contribute to errors in the acoustic system, primarily from undiagnosed temperature gradients and wave-induced water level draw-down. Water level comparison between the acoustic and microwave systems reveal that the majority of differences are accounted for by errors in the acoustic system. It is demonstrated that resonance of the protective well of the acoustic system can distort the spectral variance of water levels and that the microwave sensor captures water level variability with higher fidelity than the acoustic system when waves are present. Although the microwave system has limitations such as signal scattering and sidelobe interference, when temperature or wave forcings are present the microwave sensor is a more accurate water level gauge than the acoustic system.

Aquatrak | Microwave | Water Level Error

Introduction

The National Oceanic and Atmospheric Administration (NOAA) National Ocean Service (NOS) manages the National Water Level Program (NWLP) to meet NOAA mission requirements for coastal water level information. The NWLP is a major observational program within NOS, and serves as a Federal component of the Integrated Ocean Observing System [1] and the Global Sea Level Observing System [2]. A fundamental component of the NWLP is the National Water Level Observation Network (NWLON), a network of more than 200 long-term, continuously operating water level stations around the United States including island possessions, territories and the Great Lakes.

Since the early 1990s the primary water level measurement system at most NWLON stations has been an acoustic time-of-flight range sensor [3]. The sensor is coupled to a sounding tube that guides an acoustic pulse to the water surface. The system is self-calibrating in the sense that it monitors the effective sound speed between the transducer and an acoustic reflector at a known distance (1.219 m), thereby adjusting for temperature changes in sound speed. However, this assumes that the temperature near the transducer is representative of the mean temperature along the entire tube, and a potential error source arises from the strong temperature dependence of acoustic celerity [4, 5]. When the sounding tube is longer than a few meters and the temperature difference between the upper section of the tube and the water surface greater than a few degrees, water level errors of several centimeters are possible.

The sounding tube is further enclosed in a vented protective well, a 15.24 cm diameter pipe extending below the water surface terminated with a brass orifice to restrict water mass transport in/out of the well. The orifice is sized to work with the protective well to impose a mechanical low-pass filter on pressure-induced water level variations inside the well. The primary source of these high frequency oscillations is a natural resonance of the well to buoyancy forces driven by pressure differences at the top and bottom of the well. In addition to these water level oscillations inside the well, wave-induced hydraulic pressure changes from hydrodynamic flow across the orifice are known to draw-down or pile up water inside the well introducing another potential error [6].

From a logistical perspective, installation and maintenance of the protective well requires nontrivial infrastructure and yearly servicing including dive operations, and there is potential for the well to be damaged from flotsam or vessel impacts.

Wave Height Dependence. As surface wave amplitude increases there is an observed increase in water level standard deviation (σ), although the relationship has been viewed primarily as a source of error in the water level measurement [6, 7]. However, as part of the TOPEX/Poseidon validation experiments a direct relationship between significant wave height ($H_{1/3}$) and standard deviation was established [8, 9]. It was concluded that standard deviation of the NOAA water level estimate is a good first-order measure of significant wave height with the proviso that the protective well and low pass filter can bias the wave height estimates, and that below a threshold wave height the relationship would degrade such that in protected waters estimates of wave height would not be viable.

Given that the NWLON continuously monitors coastal water levels at numerous stations covering the United States coastline, a robust relationship between significant wave height and water level standard deviation could provide wave height estimates useful to coastal interests. Taking note of this, the Integrated Ocean Observing System (IOOS) plan for a surface-wave monitoring network recognized that non-directional wave data extracted from NLWON water level standard deviation can augment directional wave observations and are particularly useful in understanding the transformation and dissipation of waves as they traverse shallow and complex local bathymetry [10].

MWWL Phase II Analysis. The emergence of microwave water level sensors without temperature dependence or hydraulic pressure effects, and with substantially reduced installation and maintenance costs has motivated NOAA to transition from acoustic systems to microwave sensors where possible [11]. However, the microwave sensors have limitations such as signal scattering/blockage from rain or flotsam, and a variable surface area footprint dependent on sensor beamwidth and range from the water which introduces a spatial filter [12].

NOAA field evaluations comparing the two sensors find statistically equivalent performance at stations with little or no surface wave energy and small thermal gradients along the sounding tube. At stations with persistent surface waves larger than roughly 0.5 - 1 meter significant wave height, monthly mean water levels consistently reveal lower levels observed with the acoustic sensor. Boon et. al. also reported differences between the acoustic and microwave system response with wave conditions, and presented evidence of an asymmetric water level distribution when waves are present [7, 13].

To assess these differences, the *Microwave Water Level (MWWL) Phase II* project was designed to collect collocated acoustic and microwave water level data at NWLON stations where wave energy is known to be persistent [14, 15, 16, 17, 18]. Site selection was based on comparison of empirical cumulative distribution functions (ECDF) of water level standard deviation over a period of 1 year. Figure 1 shows the ECDF at select NWLON stations with coastal exposure. Bay Waveland MS and Port Townsend WA are typical of stations protected from wave energy. In the intermediate regime are Monterey CA and Lake Worth FL, while stations that represent high amplitude Aquatrak σ and wave energy include La Jolla CA, Duck NC, Wrightsville Beach NC and Santa Monica CA. Based on the ECDF analysis, four NWLON stations with intermediate and high energy wave environments were selected for Phase II data collection and analysis: Duck NC, Lake Worth FL, La Jolla CA and Monterey CA (figure 2).

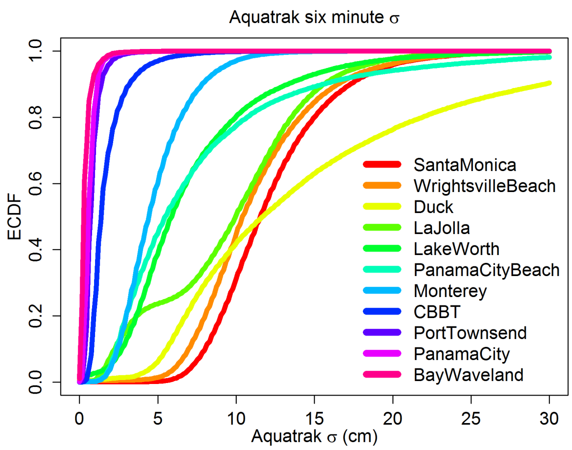

Fig. 1. Empirical cumulative distribution functions of Aquatrak DQAP σ over a period of 1 year at coastal NWLON stations.

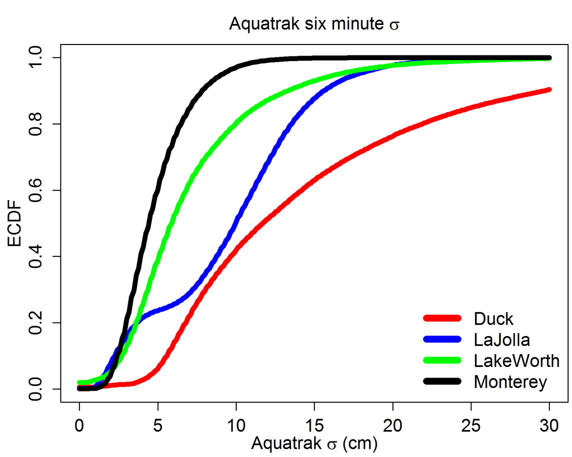

Fig. 2. Empirical cumulative distribution functions of Aquatrak DQAP σ over a period of 1 year at four NWLON stations selected for Phase II analysis.

The intent of this report is to assess comparative performance of the acoustic and microwave sensors in response to wave and temperature forcings for NOAA water level measurement, and to attribute these differences to known physical responses of the sensor systems. The following sections describe the sensors, and give particular attention to models of the leading error sources for the acoustic system. Data from Duck NC and Lake Worth FL are used to illustrate the sensor characteristics and error estimates. Supporting data from all four Phase II test sites are presented in appendix *Additional Analysis Results*.

Sensors

Acoustic Water Level. The acoustic system is described by Edwing [3] and is fundamentally a time-of-flight sensor encased in a protective well. Two temperature sensors (thermistors) are attached to the sounding tube to monitor temperatures within the protective well (discussed in section *Acoustic Temperature Dependence*). The upper sensor is close to the acoustic transducer, while the second sensor is located above the highest astronomical tide.

The protective well provides physical protection for the sounding tube as well as a mechanical low-pass filter that effectively damps high frequency water level variance. Significant effort was expended in the 1980's with a series of laboratory, field, and numerical experiments to design the protective well based on hydrodynamics of water level frequency response in the well [19, 6]. Figure 3 reproduces the dynamic water level response inside the well, R, to surface wave excitation of height H and period T from the work of Shih [19]. This response is the classic 2^{nd} order (nonlinear) frequency response function for a physical system with mass, potential and kinetic energy transfer, and damping [20].

Ignoring frictional effects and dependence of the protective well diameter, the natural (resonant) period of oscillation is $\mathrm{T_n} = 2\pi\sqrt{\frac{\mathrm{Y}}{\mathrm{g}}}$ where Y is the orifice submergence depth and g the gravitational acceleration. For typical submergence depths of 4 to 6 m at coastal locations the first order estimate of $\mathrm{T_n}$ ranges from 4 to 5 seconds. At the Duck NWLON station the orifice submergence depth is 3.9 m below mean sea level corresponding to a natural frequency of approximately 4 seconds. The damping factor is determined by the mass flow rate through the orifice and given by $\zeta = \mathrm{d_w}/\mathrm{d_o}$ where $\mathrm{d_w}$ and $\mathrm{d_o}$ are the diameters of the protective well and orifice respectively.

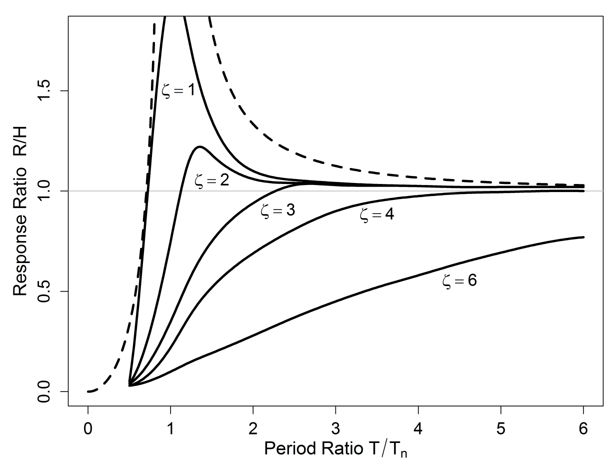

Fig. 3. Dynamic water level response (R) inside a protective well to surface waves of height H and period T. $\mathrm{T_n}$ is the resonant period of the well and $\zeta = \mathrm{d_w}/\mathrm{d_o}$ is the damping factor where $\mathrm{d_w}$ and $\mathrm{d_o}$ are the diameters of the protective well and orifice respectively. The dashed line represents the theoretical response in the absence of damping.

Examination of figure 3 reveals why the orifice has a diameter of $\mathrm{d_o} = 5.08$ cm. With a protective well diameter of

d_w = 15.24 cm the value of ζ is 3, corresponding to a critically damped response. It is important to realize that figure 3 represents the response to a specific set of parameters: H = 0.3 m, orifice submergence depth 3.0 m, water depth 7.6 m. Changing these parameters alters the shape and amplitude of the response curves and it is obvious that the single system design represented in figure 3 will behave quite differently under varying parameter regimes. For example, increasing the orifice submergence depth increases the amplitude response R near resonance ($T = T_n$).

Another primary investigation by Shih concerned wave-induced pressure variations which draw-down water level inside the well. This is a concern at stations where tidal currents are significant, or when surface waves drive pressure oscillations and subsurface flow. This effect was quantified by Shih & Rogers [6] as a function of wave height and period as shown by the functional relationship in figure 4. One can use this function to asses water level differences between the microwave and acoustic systems in response to wave forcing. Again, it should be noted that while this curve applies to general combinations of wave height and period, protective well and orifice diameter; it is specific to an orifice hydraulic discharge coefficient of $C_d = 0.8$, orifice submergence depth 3 m, and water depth of 9.14 m. Deviations from this parameter regime will alter the response of this model.

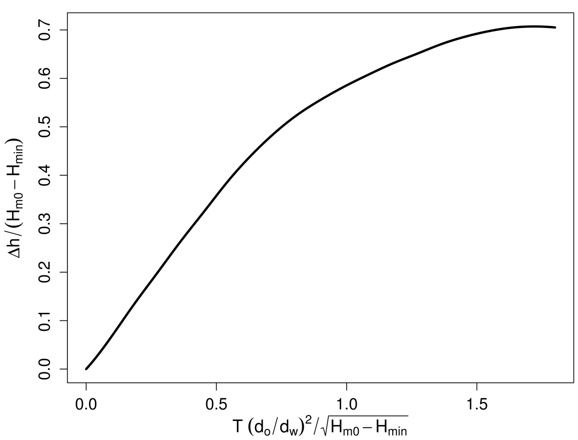

Fig. 4. Relationship between water level draw-down in centimeters (Δh) and surface wave forcing. T is the wave period, d_o/d_w the ratio of orifice to protective well diameter, H_{m0} the significant wave height in meters, and H_{min} a minimum threshold wave height below which wave effects are not important.

As referenced earlier, when wave energy increases standard deviation of water level estimates also increase. Parke & Gill [9] evaluated this dependence for the acoustic system as part of the TOPEX/Poseidon validation at Platform Harvest finding a linear increase of water level standard deviation with values in the range of 10 - 20 cm for significant wave height of 1 m. This is consistent with data presented in sections *Water Level Standard Deviations and Significant Wave Height* and *Additional Analysis Results*. For example, at Duck North Carolina standard deviation values in the range 7 - 20 cm correspond to significant wave heights of 1 m.

Microwave Water Level. The microwave sensor operates at a frequency of 26 GHz with a beamwidth of 8 to 10° depending on the antennae. There is no contact with the water surface and no dependence on pressure, hydrodynamic flow, or density of the water. The sensor is remarkably insensitive to temperature variation (0.2 mm/°K, 5 mm maximum) and has accuracy of ±0.03% of the measured range. Details of the sensor can be found in the NOAA Limited Acceptance Test Report [21]. Boon et al. [7] estimated sensor accuracy for NOAA water level estimates finding a quadratic increase of sensor error with wave height. They also identified an asymmetric distribution of water levels when wave height increased. This asymmetry is consistent with the development of a Rayleigh distribution of water level in the presense of waves.

Data

As mentioned above, the MWWL Phase II project targeted four NWLON stations for data collection and analysis: Duck NC, Lake Worth FL, Monterey CA and La Jolla CA. The data period spans April 2012 through November 2013. Raw range to water data were sampled from both the microwave and acoustic sensors at 1 Hz. This raw 1 Hz data is used in power spectral density (PSD) estimates and to estimate range to water by application of the NOAA Data Quality and Assurance Procedure (DQAP) [22]. This algorithm samples 181 consecutive 1 Hz values centered on each hour and 6 minute interval (minutes 0, 6, 12, 18, 24, 30, 36, 42, 48, 54) to compute an initial mean and standard deviation. Data points greater than 3 standard deviations from the mean are discarded, and a final mean and standard deviation are computed from the remaining points. These range data are transmitted by satellite to NOAA's Center for Operational Oceanographic Products and Services (CO-OPS), where they are converted to water level by subtracting the range estimates from the reference datum, which are then disseminated in near real time on the Internet and stored in the NWLON archives.

An example of the data for April 2012 at Duck is shown in figure 5 where the upper panel plots the difference between the hourly acoustic and microwave water levels, the middle panel the temperature difference between the two thermistors, and the lower panel significant wave height. The water level differences are acoustic - microwave, so that a positive differential implies the acoustic system reported a higher water level, a negative one that the acoustic level is lower. The temperature differences are upper thermistor - lower thermistor, such that a negative differential represents a higher temperature along the sounding tube than at the acoustic transducer.

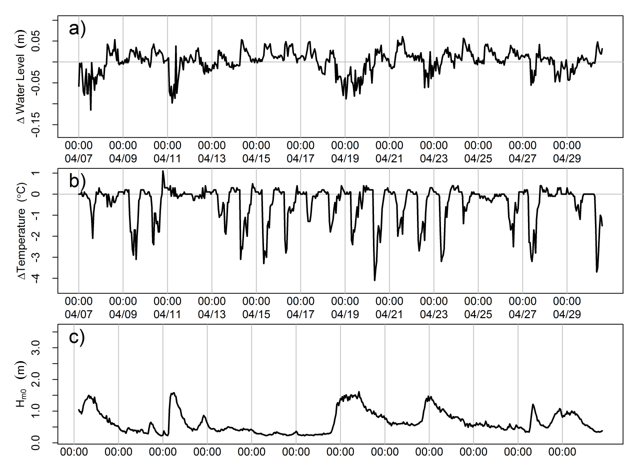

Fig. 5. Hourly data from Duck North Carolina in April 2012. a) DQAP water level difference between the acoustic and microwave sensors. b) Temperature difference between the upper and lower thermistors of the acoustic sounding tube. c) Significant wave height. Times are Coordinated Universal Time (UTC).

Two inferences are apparent from examination of figure 5. Positive water level differences are related to negative temperature differentials along the sounding tube, and negative water level differences are related to significant wave height. Each of these observations is examined in the following sections, but first let us establish some general characteristics of the sensors with spectral analysis.

Acoustic and Microwave Frequency Response

Examination of water level power spectral density (PSD) estimates under different wave conditions reveals some fundamental response characteristics of the two systems. PSDs are estimated from raw 1 Hz water level data with a periodogram smoothed by a modified Daneill smoother of span 600 points resulting in a spectral amplitude 99% confidence interval of 1.1 dB. Resultant PSDs for four distinct wave regimes are shown in figure 6. Panels a, b and c show spectra from waves of increasing height, all with dominant wave periods in the 7 to 15 second range. Panel d plots the response to a short period (4.1 second) wave field generated by the passage of a cold front on April 27 2012 (discussed in *Standard Deviation and Significant Wave Height*).

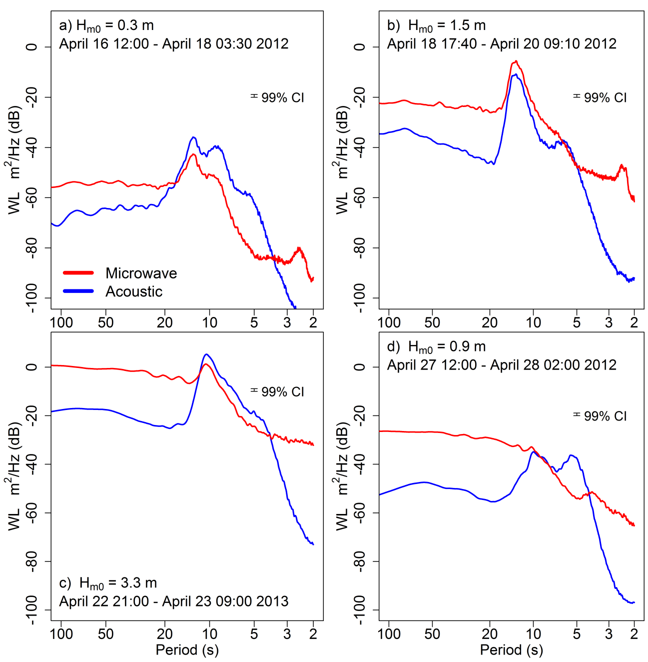

Fig. 6. Power spectral density estimates of 1 Hz water level data from the acoustic and microwave sensors at Duck NC. a) Low wave conditions. b) Intermediate to high wave conditions. c) Very high wave conditions. d) A locally generated, short duration swell with a dominant period of 4.1 seconds.

Perhaps the most obvious characteristic is high frequency attenuation of the acoustic system at periods shorter than about 5 seconds owing to mechanical filtering from the water inlet orifice. Another robust feature observed across multiple data sets and environmental conditions is enhanced response of the microwave sensor to water level variance from low to intermediate/high wave conditions in the wind wave frequency band (periods of 5 to 20 seconds). This can be seen by comparison of panels a and b. In panel a the wave height is low and the microwave sensor water level variance is 5 to 10 dB less than that of the acoustic system in the wind wave band. In panel b the wave height has increased by a factor of 5 and one finds the microwave water level response is roughly 5 dB greater than that of the acoustic system. This 'inversion' of water level variance translates into a superior water level sensitivity for the microwave sensor in the low to intermediate/high wave regime, and led to identification of the microwave sensor as a higher fidelity water level sensor in the presence of waves (discussed in *Standard Deviation and Significant Wave Height*).

Although the sensitivity of the microwave sensor to water level dynamics is greater than the acoustic system for low to intermediate/high wave conditions, we see in panel c that when waves are very high the acoustic sensor reports higher variance in the 4 to 12 second band. NOAA is continuing to collect and analyze data in the high wave regime to ascertain if this is a consistent characteristic between the two sensors.

Resonance of the protective well is a notable feature in panel d. It is clear that the 4.1 second dominant wave period is captured by the microwave sensor, while the acoustic system responds with a broad peak centered on a period of 5 seconds. This can also been seen in panel a, where the acoustic spectra has a 'knee' at a period of 5 seconds while the microwave presents no such energy. It is also likely that the broad peak centered on a period of 5 seconds in panel b can be attributed to the protective well resonance.

Data from Lake Worth FL shown in figure 7, where short period surface wave energy is common, show extreme distortions of spectral amplitude due to this resonance (see also figures 33 and 35 in *Additional Analysis Results: Lake Worth*). That this resonant spectral energy is a distortion is verified by the lack of coherence between the acoustic and microwave water levels spanning the period of the protective well resonance. These distortions have potential to bias the water level estimates since they represent energy inside the protective well due to resonance, not variance due to the true dynamics of the water surface.

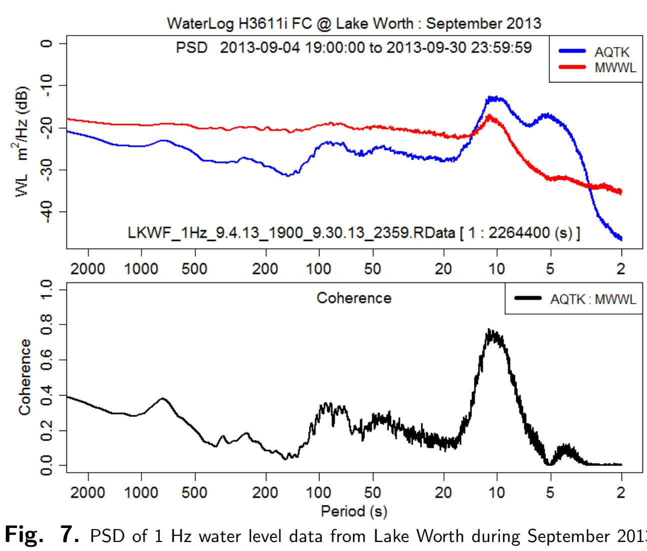

Fig. 7. PSD of 1 Hz water level data from Lake Worth during September 2013. Resonance of the protective well is presented as a large distortion of the spectral variance centered on a period of 5 seconds. The lack of coherence between the acoustic and microwave water levels at 5 seconds indicates that this resonant energy is a distortion.

These resonance features are consistent with the dynamic response of the protective well being forced by combinations of parameters (wave height and period, orifice submergence depth, water depth, orifice discharge coefficient etc.) which deviate from the ideal design represented in figure 3 such that the critically damped response is not realized.

At periods longer than 20 seconds the microwave sensor consistently measures higher water level variance than the acoustic system. At these long periods we are no longer dealing with direct-wind generated ocean surface waves, but are sampling infragravity waves and other nonlinear processes associated with subharmonics of wind waves, internal waves, edge-waves trapped on the shelf, or other forcings [23]. It is not presently known whether this response represents a higher fidelity sampling of low frequency variability, a limitation imposed by the acoustic system mechanical filter or microwave sensor, or some other effect. However, a consistent feature is that the shape of the spectral coherence at these long periods generally follows the shape of the acoustic spectra. This suggests that the protective well affords some level of noise-rejection at very low frequencies. Nonetheless, values of coherence at these long periods is consistently low, indicating systemic differences in the sensing modalities of the two sensors.

Acoustic Temperature Dependence

In previous work investigating the relationship between temperature and accuracy of the acoustic ranging system Porter et al. described the system, the presently used correction algorithm, and assessed impacts with a case study at the La Jolla California tide station [4]. Their data reveal water level errors of the order of 5 cm arising from temperature-induced sound speed errors. Hunter conducted a comprehensive analysis of the temperature dependence, again finding the dominant error arising from uncertainty in sound speed [5].

It is worth noting that the current NWLON temperature correction algorithm makes a significant assumption concerning representation of the physical environment. The correction is:

$$\Delta S = 0.0018\, h\, \Delta T \qquad [1]$$

where ΔS is the water level correction, h is the range from the acoustic transducer to the water surface and ΔT the difference between the temperature measured near the transducer and the temperature measured closer to the water surface. The factor 0.0018 is a constant relating the sound speed in an adiabatic ideal gas to temperature in units of degrees Celsius.

This correction contains no dependence on the location of the temperature measurements. For example, for a given range to the water h, the correction ΔS computed from ΔT measured over a distance of 1 cm is the same as for ΔT measured over a distance of 10 m. The assumption is that a step-wise constant temperature difference, one temperature at the sensor and another constant temperature along the sounding tube, accurately represents the effective temperature profile along the sounding tube. This first-order assumption may be valid in certain cases, however, in cases where the actual temperature profile is not well represented by a spatially independent temperature difference, the correction from equation 1 is known to be poor [24, 25]. NOAA is currently exploring the use of additional thermistors and a spatially dependent algorithm to improve sound speed corrections. Note that for the data analyzed here, temperature corrections exceeding 5 cm are not uncommon.

As previously noted from inspection of figure 5, a relation between positive water level differences of the acoustic and microwave sensors and negative temperature difference of the two thermistors is evident. Even though the temperature correction of equation 1 is based on a simplistic physical model, it is the currently accepted algorithm and it is used to compute temperature corrections for the data shown in figure 5. These corrections are then compared with the observed water level differences as shown in figure 8. The acoustic temperature corrections are largely coherent with the positive water level differences with pronounced disagreement primarily arising when significant wave height is greater than 0.5 m. These discrepancies are attributed to increased thermal mixing within the protective well driven by wind stress and pneumatic pumping from water level variance since the protective well is vented at the top to allow ambient pressure equalization. The extent to which these positive water level differences are captured by the correction of equation 1 can be examined with linear regression of the positive sea level differences with the temperature corrections for data having wave height below a certain threshold. With a threshold of $H_{m0} < 0.5$ m the regression finds a linear dependence of $c = 0.86$ with $r^2 = 0.49$ $(p < 1E-9)$, where c is the regression coefficient and p the p-value.

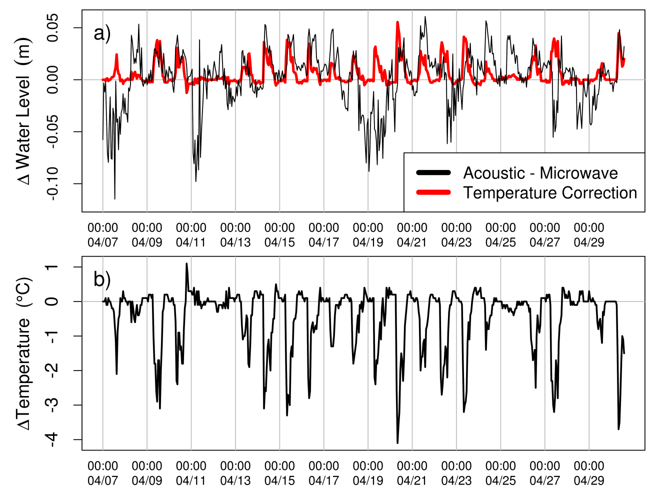

Fig. 8. Hourly data and temperature corrections from Duck in April 2012. a) Water level difference between the acoustic and microwave sensors (black) and acoustic temperature water level error estimates (red). b) Temperature difference between the upper and lower thermistors of the acoustic sounding tube.

This data, along with data presented in *Additional Analysis Results* confirms that temperature-induced errors of acoustic water level are a significant disadvantage of the acoustic system in relation to the microwave system.

Mechanical Filter Water Level Draw-Down

To evaluate water level draw-down in the acoustic system the functional relation of figure 4 is applied to the data of figure 5, with results presented in figure 9. One can see that the envelope of the draw-down model captures the overall negative water level differences, however, there are differences at short time scales (several hours) as positive water level differences are observed during wave events, for example during the period April 11, 2012. It is not known whether these positive water level differences represent an error of the microwave sensor when water level variability is high [7], or whether it is a response of the acoustic system protective well and orifice. Given the nonlinear response of the of the protective well to wave forcings, and known issues of water level pile up in the well, it is likely that these short timescale differences are driven by resonance of water levels from a loss of damping in the acoustic system protective well.

To assess the draw-down model one can regress the envelope of negative water level differences against the predicted draw-down. The water level difference envelope is obtained from low pass filtering the magnitude of the differences with an 18 hour moving average filter and the result is $c = 0.30, r^2 = 0.55$ ($p < 1E-9$). Copious examples of water level draw-down driven by wave-induced hydrodynamic flow are presented in *Additional Analysis Results*.

Not accounting for wave-driven water level reductions in the acoustic sensors can impact long term water level statistics. For example, by integrating the negative water level differences in figure 9 the reduction in mean sea level between the acoustic and microwave water levels over the April 2012 record is estimated to be 1.1 cm. This closely matches the observed difference in sensor range shown by probability densities of the sensor range differences in figure 10. Probability density functions (PDF) were computed based on subsets of the range data partitioned according to three regimes of DQAP standard deviation: Low ($0 < \sigma < 1/3$), Med ($1/3 < \sigma < 2/3$) and High ($\sigma > 2/3$).

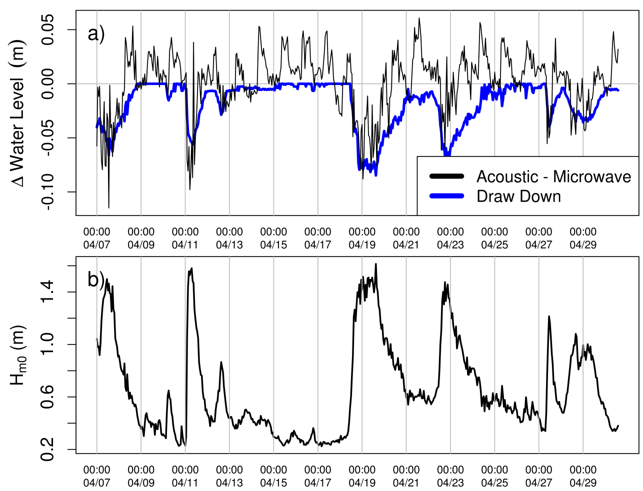

Fig. 9. Hourly data and draw-down corrections from Duck in April 2012. a) Water level difference between the acoustic and microwave sensors (black) and protective well draw-down estimates (blue). b) Significant wave height.

Two additional observations from the probability densities are that in Fast Change mode, modal values of the partitioned PDFs are conserved, and that as σ increases the tail of the PDF increases for negative range to water levels. The former observation validates stability of the microwave sensor mean estimates with respect to the Aquatrak as a function of water level energy, while the latter suggest the emergence of an asymmetric water level distribution consistent with the transition from non-wave (Gaussian) to wave water level statistics (Rayleigh). Fast Change is a microwave sensor mode that implements internal smoothing with a time constant of approximately 5 seconds, while No Filter mode reports raw range values. Fast Change mode is the default CO-OPS operational mode [21]. See figure 22 in *Additional Analysis Results* for a comparison of Fast Change to No Filter sensor modes.

These differences are consistent with the monthly mean differences which motivated the restriction of microwave sensors to limited-fetch, low wave energy environments. It should also be noted that in *Standard Deviation and Significant Wave Height*, comparisons of both the acoustic and microwave systems with independent water level measurements from local wave gauges show that the microwave system captures water level variability with higher fidelity than the acoustic system.

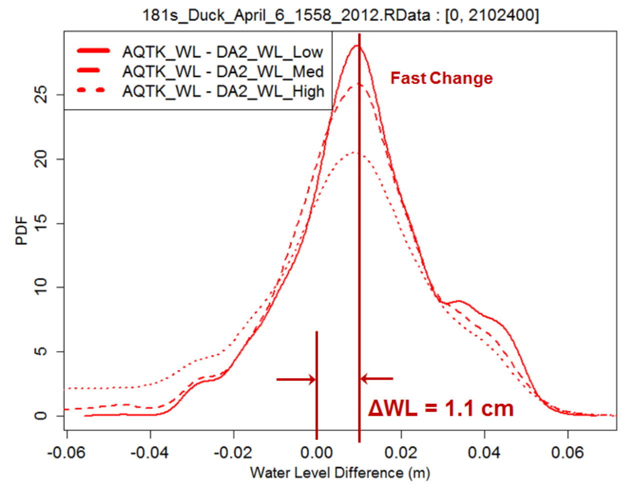

Fig. 10. Probability density functions of range to water difference (acoustic - microwave) for April 2012 at Duck. Density functions are shown for low ($0 < \sigma < 1/3$) medium ($1/3 < \sigma < 2/3$) and high ($\sigma > 2/3$) partitions of the data.

Based on the data presented here and in *Additional Analysis Results*, it is clear that the acoustic system is poorly suited for environments with significant tidal or wave-induced hydrodynamic flows. At stations where these conditions prevail, the microwave sensor provides water level estimation with higher accuracy than the acoustic system.

Standard Deviation and Significant Wave Height

A comparison of wave gauge hourly Hm_0 with water level standard deviations of the acoustic and microwave gauges over 24 days in April 2012 at Duck is shown in figure 11, suggesting a robust relationship between wave height and water level standard deviation.

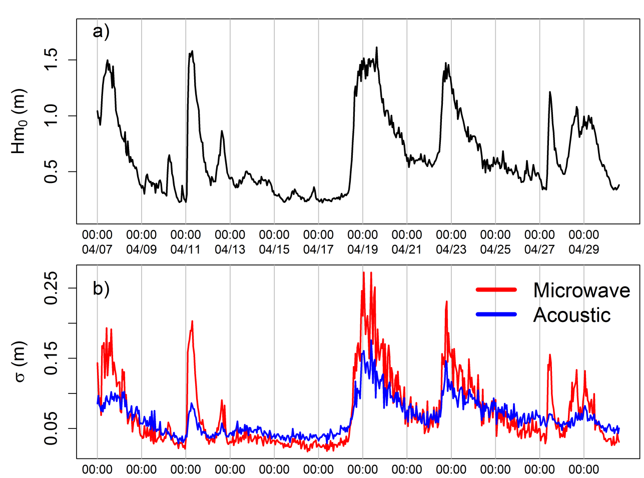

Fig. 11. a) Hourly significant wave height (Hm_0) during a 24 day period in April 2012 at the Duck North Carolina b) Hourly NWLON standard deviations.

Direct estimation of Hm_0 from σ would utilize the canonical definition:

$$\mathrm{Hm}_0 = 4\,\sigma. \qquad [2]$$

However, one can recognize that several factors contribute to deviations from this ideal. One is that we are relating Hm_0 estimated from the AWAC gauge over a period of 1 hour with a single σ estimated over 181 seconds. Other factors include the spatial separation between the wave gauge and water level sensors, and water level measurement system mechanics, e.g. the acoustic protective well introduces nonlinear filter to the water level variance and this response is known to depend on wave height, period, and water depth [6]. Further, the microwave sensor images a variable footprint on the water surface depending on the sensor to water distance, and implements some internal smoothing of the 1 Hz data. Therefore, it is not expected that NWLON water level σ will explicitly satisfy equation 2, but can hope for a linear scaling and seek a parameter α that best relates water level σ to Hm_0:

$$\hat{\mathrm{Hm}}_0 = \alpha\,\sigma \qquad [3]$$

where $\hat{\mathrm{Hm}}_0$ is the estimate of Hm_0 and α a factor which minimizes the residual $\epsilon = \mathrm{Hm}_0 - \hat{\mathrm{Hm}}_0$. Fitting a linear model over the 24 day period results in $\alpha_\mu = 6.53$ and $\alpha_\mathrm{A} = 11.08$ for the microwave and acoustic sensors respectively with the resulting wave height estimates $\hat{\mathrm{Hm}}_0$ shown in figure 12. The mean error of these first-order estimates can be represented with the RMS residual over the period and finds values of $\epsilon_\mu = 0.14$ m and $\epsilon_\mathrm{A} = 0.21$ m for the microwave and acoustic sensors.

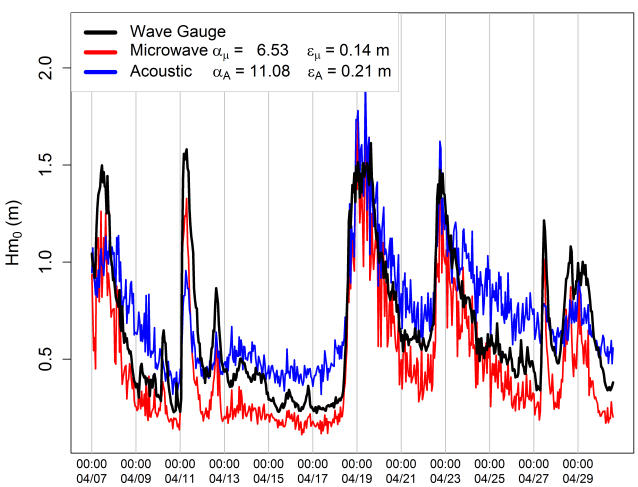

Fig. 12. Hourly significant wave height (Hm_0) and estimates of wave height ($\hat{\mathrm{Hm}}_0$) from a linear model of Hm_0 regressed onto water level standard deviations (σ) over 24 days of April 2012 at the Duck. α is the fit coefficient, ϵ the RMS residual between wave gauge Hm_0 and estimated wave height ($\hat{\mathrm{Hm}}_0$).

To assess the dynamics of this linear scaling on a finer temporal scale one can regress hourly Hm_0/σ over a sliding window of length 24 hours with the the resultant fit and correlation coefficients shown in figure 13. Correlation and fit coefficients are only shown if the p-value of the fit exceeds the 99% confidence level. The dashed line quantifies an ideal model of $\mathrm{Hm}_0 = 4\,\sigma$, and we see that in a linear least squares sense the microwave sensor comes closer to this definition than the acoustic sensor. Both models find a significant dependence (p-values < 0.01) during times of wave activity, note that in concordance with the expectation of Parke & Gill [9] when wave activity is low (days 14, 17, 24-27) the model fails to be statistically significant, although there are a exceptions (days 9 and 30). Generally, the predictive skill of the acoustic system is less robust than that of the microwave system with consistently lower r^2 values and fit coefficients farther away from the ideal.

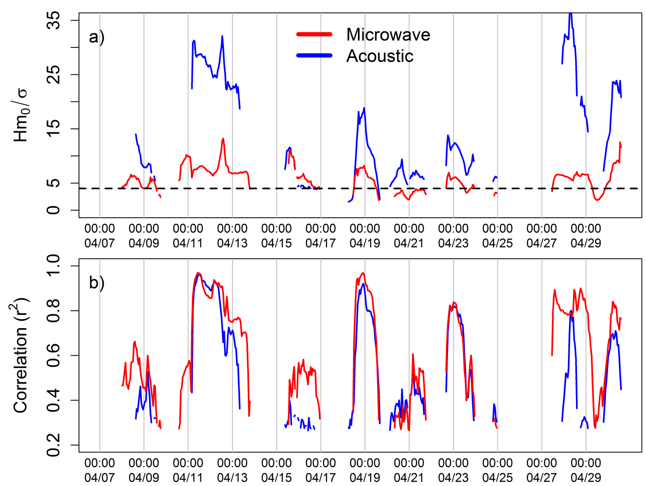

Fig. 13. Linear regression of significant wave height (Hm_0) onto microwave and acoustic standard deviations shown in figure 11 over a 24 hour sliding window. a) Fit coefficients. The dashed line shows the ideal model of $\mathrm{Hm}_0 = 4\,\sigma$, corresponding to the accepted definition of significant wave height. b) Correlation coefficients. Values are shown only if the p-value exceeded the 99% confidence level.

A re-examination of the acoustic and microwave water level σ shown in figure 11 reveals that the microwave sensor exhibits a greater dynamic range than the acoustic system. During times of low σ the microwave response is lower in amplitude than that of the acoustic system, whereas during time of high σ the microwave response is higher. This suggests that in terms of water level variations the microwave sensor has a higher sensitivity than the acoustic system consistent with the spectral analysis presented in *Acoustic and Microwave Frequency Response*.

Another difference evidenced in figure 11 during day 27 is that microwave sensor exhibits a pronounced response to a short-term wave event while the acoustic system presents only a minor indication. Examination of meteorological data [28] reveals that a cold front moved through the area on April 27 with a change in wind direction from 270° to 10–60° (offshore to onshore) with wind speeds during the period increasing from 5 to 10 m/s (10 to 20 knots). These conditions are consistent with the formation of locally-generated, short-period wind waves. Wave gauge records over this period reveal an average wave direction of 64°, height of 0.9 m, and period of 4.1 s. Water level PSDs encompassing this event are shown in panel d of figure 6 and we observe that at periods between 2 and 4 seconds, the acoustic system is attenuated from the low-pass mechanical filter by roughly 20 dB in relation to the microwave response, an amplitude ratio of 10 to 1. The microwave response reveals a small (3 dB), but statistically significant broad peak between 3 and 5 seconds corresponding to the wave gauge report of a 4.1 second period.

The combination of meteorological, wave gauge, and water level PSDs suggests that the wave event on April 27 was primarily locally-generated, short-period wind waves that the acoustic system filtered out, but which drove the protective well into a resonant water level oscillation at a period of 5 seconds. This resonance introduces distortion into the spectral variance, and at some point will contribute to increased error of the water level estimate.

Discussion

As part of a modernization effort for NOAA's National Water Level Observation Network, acoustic ranging water level systems are being transitioned to microwave radar sensors. From a cost, maintenance and support perspective the microwave sensor is more efficient than the acoustic system since it requires no infrastructure in contact with the water, although it has limitations to be considered. When used without a protective well, flotsam or surface ice can lead to erroneous water levels. It is also known that ice accumulation in the antennae as well as scattering from heavy rain can degrade sensor performance. The use of a protective antenna cover (end cap) to prevent ice buildup inside the antenna does effectively mitigate the ice problem, but introduces another where moisture accumulation on the cover impedes the signal [26]. The microwave beampattern also needs evaluation to ensure that interference from pilings/mounting structures does not impede imaging the water surface, and in surface wave sensing applications the footprint of the beam introduces a spatial filter [12].

Two benefits of the microwave sensor are that it is insensitive to temperature, and does not rely on a hydraulic pressure measurement. With regard to temperature effects, the analysis finds that from 1/2 to 2/3 of water level differences between the acoustic and microwave sensors can be attributed to speed of sound errors in the acoustic system. An improved temperature correction algorithm would find higher proportions. Temperature errors of 5 cm and greater are common at La Jolla and Duck, as are temperature errors of 2 to 4 cm at Lake Worth (*Additional Analysis Results*).

When a wave-induced water level draw-down model for the acoustic protective well is applied, the analysis finds that 1/2 to 3/4 of the negative water level differences can be attributed to wave-induced pressure changes. Even though differences in water level response as a function of wave height are reasonably captured by the hydrodynamic draw-down in the protective well, there are exceptions during high wave events when a water level pile up is observed. Based on the nonlinear response of the protective well, a leading hypothesis for these observations is resonance of the protective well due to a loss of damping. Further study is needed to clarify this behavior.

Spectral analysis demonstrates that resonance of the protective well can introduce large distortions to water level variance centered on periods of 5 seconds. Suppression of this resonance was a primary objective of the orifice and low-pass filter, however the highly dynamic and variable parameter regimes of the nearshore wave zone can invalidate assumptions inherent in the one-design protective well. These distortions have potential to bias the water level estimate, and further study is needed to identify the extent of such impacts.

NWLON data products recorded every six minutes include the standard deviation (σ) of 181 water levels sampled at 1 Hz. The σ statistic is known to be correlated with significant wave height, but has been largely ignored as a wave height measure and viewed primarily as an error metric of water level estimates. To assess the link between water level standard deviation and significant wave height a linear model significant at the 99% confidence level finds that the microwave sensor estimates significant wave height, and therefore water level variability, with higher fidelity than the acoustic system.

Conclusion

The MWWL Phase II project has collected collocated acoustic and microwave water level data at four NWLON stations on both the Pacific and Atlantic coasts in intermediate and high wave environments. The data analyzed here cover the period from April 2012 through November 2013.

Data from Monterey fail to show any significant differences between the sensors due to the temperate climate, shielding of the protective well from insolation, and low waves (*Additional Analysis Results*). The other three stations (La Jolla, Duck and Lake Worth) provide consistent results which can be encapsulated as: The majority of water level differences between acoustic and microwave sensors are attributed to systemic errors of the Aquatrak system. The leading errors are:

1. Speed-of-sound errors from undiagnosed temperature gradients along the sounding tube.
2. Water level draw-down errors from wave-induced hydrodynamic flow across the protective well orifice.
3. Resonance of the water level inside the protective well from buoyancy driven pressure fluctuations.

The microwave sensor is insensitive to temperature, and is not influenced by hydraulic pressure as is the case for pressure sensors, and for water level inside the Aquatrak protective well. It is also shown that the microwave sensor measures water level variance in medium and high wave conditions with higher fidelity than the acoustic system.

Although the microwave sensor has significant advantages, there are important performance issues to be considered including beampattern, signal scattering, blockage and false targets. Further research is needed to attribute increased water level variance measured by the microwave sensor at periods exceeding the wind-wave band (20 seconds), and additional work is also needed to clarify the positive water level differences (pile-up) when waves are very high.

In summary, the data analyzed here spanning 19 months at stations on the Pacific and Atlantic coasts demonstrate that when wave or temperature forgings are present the microwave sensor exhibits superior performance as a water level sensor in comparison to the Aquatrak.

Appendix: Additional Analysis Results

Duck

The Duck NWLON station is located at the U.S. Army Corps of Engineers Field Research Facility (FRF) [27]. A map and description of the test setup is given in Boon et al. [7]. The work by Boon et al. is the continuation of several years of microwave sensor deployments at Duck, which contributed valuable data characterizing response of the microwave sensors in a high wave environment [13].

The microwave sensor is located 8.66 m above mean water so that one can expect a single measurement accuracy of 2.6 mm. The acoustic sensor is located 7.0 m above mean water level and is calibrated to a single range measurement accuracy of 3 mm when there is zero temperature gradient between the sensor and water. Hourly significant wave height (H_{m0}) and period were obtained from a bottom mounted acoustic waves and current (AWAC) sensor operating at 1 MHz deployed on the same depth contour as the acoustic and microwave sensors (6 m) but located approximately 500 m northward.

PSD estimates of 1 Hz water level data from April 6 - 30, 2012 are shown in figure 14. Spectral features are consistent with the other data with high coherence in the wind-wave band. The low-pass filter response of the protective well is evident.

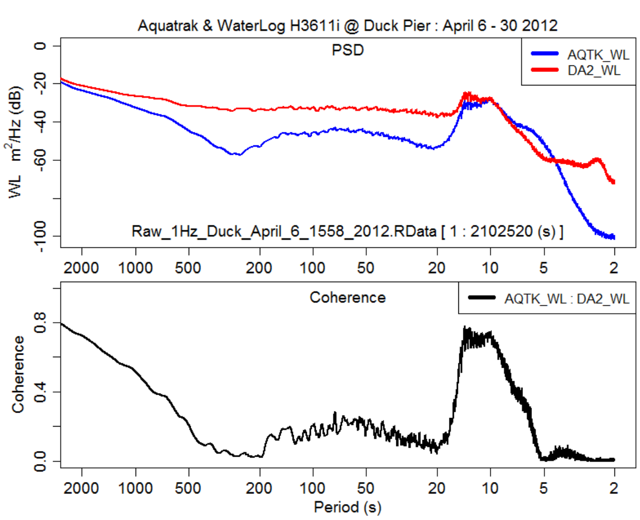

Fig. 14. PSD and coherence of acoustic and microwave water level data at Duck NC in April 2012.

PSD estimates of 1 Hz water level data from February 1 - 18, 2013 are shown in figure 15. Spectral features are consistent with the other data with high coherence in the wind-wave band and a significant distortion from the protective well resonance that is incoherent with the microwave data.

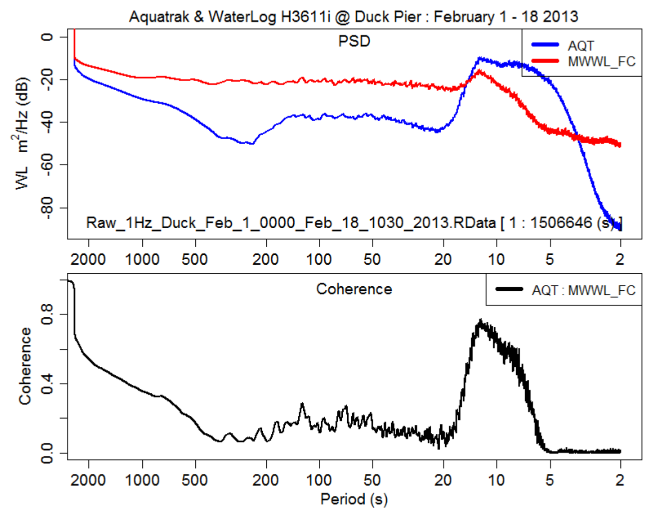

Fig. 15. PSD and coherence of acoustic and microwave water level data at Duck NC for February 1 - 18 2013.

Application of the wave draw-down model (figure 4) for data covering February 1 - 18, 2013 at Duck is shown in figure 16. With the exception of the large positive water level difference at the peak of the wave event early on February 8, the draw-down model captures the water level differences quite well and water level differences exceeding 5 cm are common. The large positive water level difference exceeds 10 cm and occurs during a period of extreme wave heights, $Hm_0 \approx 4$ m, an area that needs additional investigation. However, there is little doubt that water level measurement in the presence of 4 m waves challenges the state-of-the-art in water level estimation. The leading hypothesis at this point is a pile-up of water level inside the well due to extreme pressure fluctuations driving the nonlinear resonant response of the well. The large spectral distortion at the resonant period of the well (figure 15) supports this hypothesis.

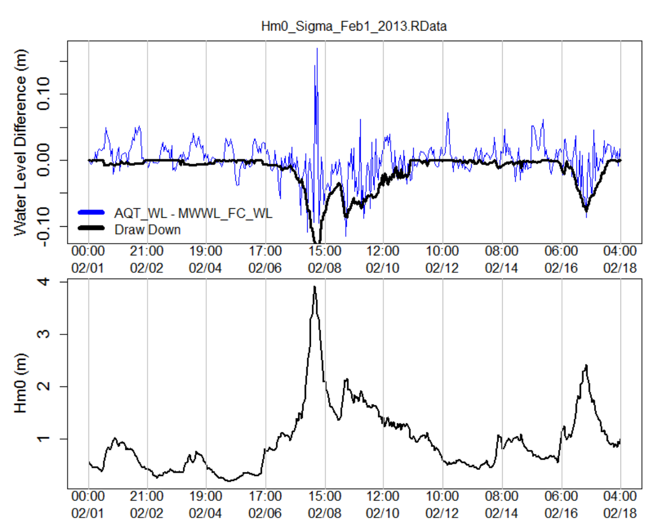

Fig. 16. Water level difference (acoustic - microwave, blue) and water level draw-down estimate (black) and significant wave height at Duck NC for February 1 - 18 2013.

PSD estimates of 1 Hz water level data from February 18 - 28, 2013 are shown in figure 17. Spectral features are consistent with the other data with high coherence in the wind-wave band and a significant distortion from the protective well resonance that is incoherent with the microwave data.

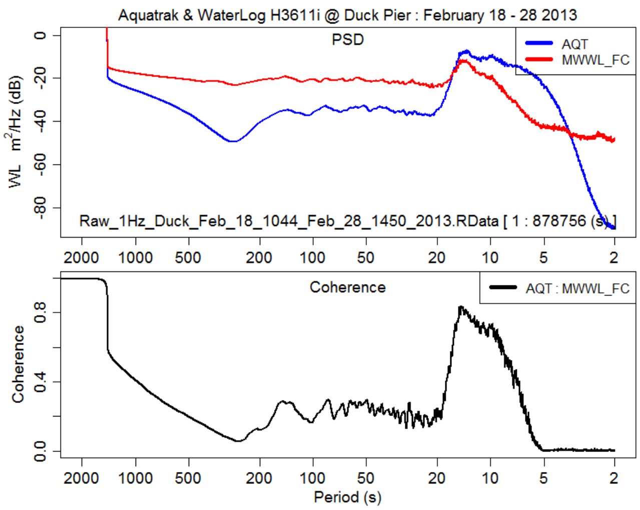

Fig. 17. PSD and coherence of acoustic and microwave water level data at Duck NC for February 18 - 28 2013.

Application of the wave draw-down model (figure 4) for data covering February 18 - 28, 2013 at Duck is shown in figure 18. The draw-down model captures the negative water level differences with good accuracy. The large spectral distortion at the resonant period of the well (figure 17) suggests that the acoustic water levels will be highly variable and this is thought to contribute to deviations from the draw-down model.

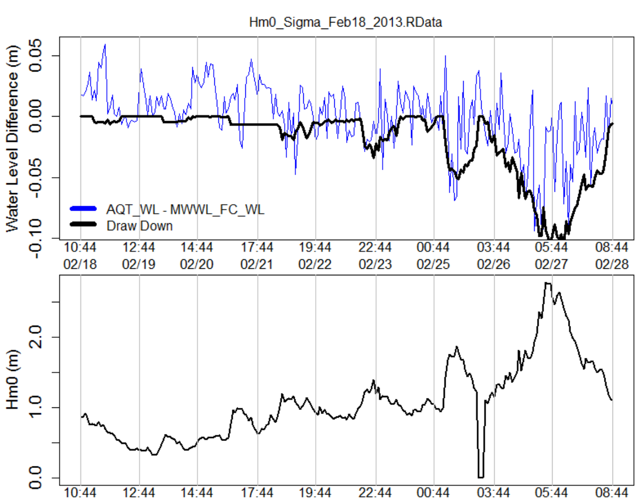

Fig. 18. Water level difference (acoustic - microwave, blue) and water level draw-down estimate (black) and significant wave height at Duck NC for February 18 - 28 2013.

Figure 19 plots sensor water level difference, acoustic temperature difference, and significant wave height for April 2013 at Duck. During times of low wave energy ($Hm_0 < 1$ m), positive water level differences are consistent with the temperature differentials. During periods of significant wave activity negative water level differences are largely coherent with significant wave height. However, during periods of high waves positive water level differences are observed.

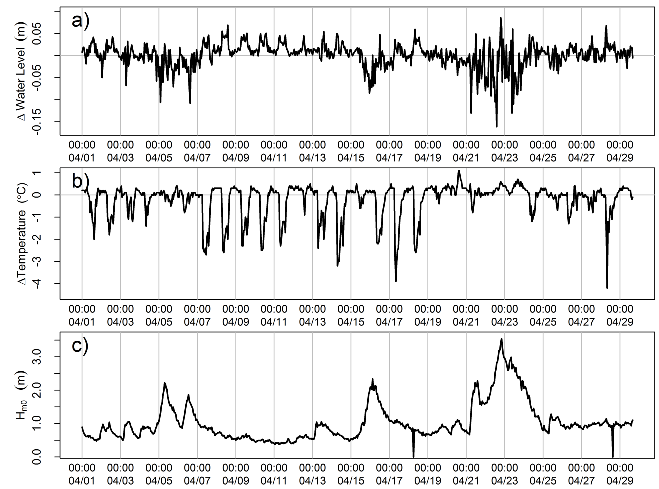

Fig. 19. Hourly data from Duck North Carolina in April 2013. a) Water level difference between the acoustic and microwave sensors. b) Temperature difference between the upper and lower thermistors of the acoustic sounding tube. c) Significant wave height.

Application of temperature corrections (equation 1) for the data shown in figure 19 are presented in figure 20. During periods of low waves temperature corrections account for the majority of the positive water level differences with a linear regression of $c = 0.82$, $r^2 = 0.59$ ($p < 1E-9$).

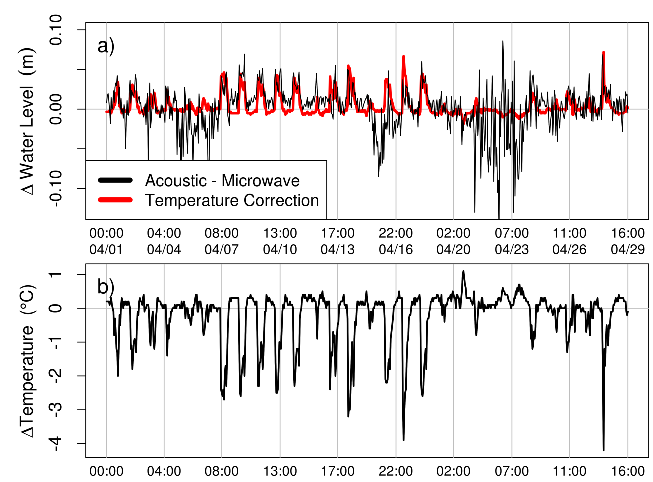

Fig. 20. Hourly data and temperature corrections from Duck North Carolina in April 2013. a) Water level difference between the acoustic and microwave sensors (black) and acoustic temperature water level change estimates (red). b) Temperature difference between the upper and lower thermistors of the acoustic sounding tube.

Figure 21 plots sensor water level differences with wave draw-down estimates, and significant wave height at Duck in April 2013. The envelope of the draw-down model captures the behavior of the negative water level differences with some exceptions, particularly when wave heights are high. Regression of low-pass filtered water level differences with the draw-down model find $c = 0.31$, $r^2 = 0.76$ ($p < 1E-9$).

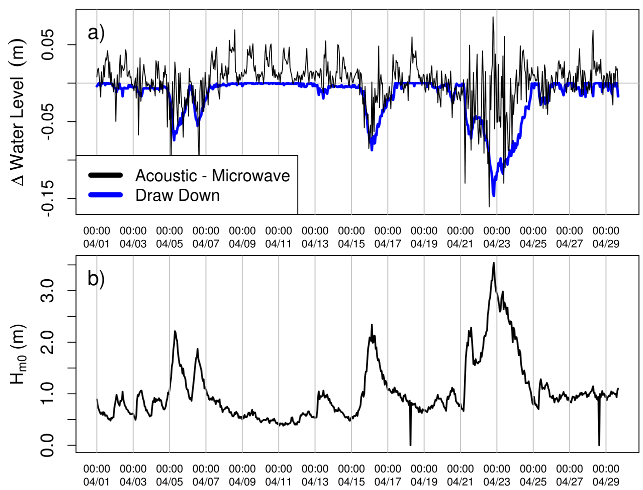

Fig. 21. Hourly data and draw-down corrections from Duck North Carolina in April 2013. a) Water level difference between the acoustic and microwave sensors (black) and protective well draw-down estimates (blue). b) Significant wave height.

One of the objectives of Phase II testing was to evaluate the microwave sensor in two different internal operating modes: Fast Change and No Filter [14, 15]. In No Filter mode the sensor reports raw range data, while in Fast Change mode the sensor implements a low-pass filter with a time constant of roughly 5 seconds. Fast Change mode is the standard operating mode for CO-OPS deployments as recommended by the Limited Acceptance Report [21]. Figure 22 presents probability density function estimates of range to water level differences for April 2013 for both No Filter and Fast Change modes. The data were partitioned into Low, Medium and High subsets based on DQAP standard deviation (σ).

Several pertinent observations can be made. First, the bias of the Fast Change distributions (1 cm) matches the estimated difference in mean water level from the draw-down model. Second, Fast Change mode preserves modal values of the probability distributions, while No Filter mode introduces a peak probability dependence on water surface variance. The reason for this modal invariance is not known, but it does support the recommendation of the Limited Acceptance Report to deploy microwave sensors in Fast Change mode, *if the Aquatrak is assumed to be a valid reference.* Since it has been shown that the microwave sensor in Fast Change mode provides a better estimate of water level variance than the Aquatrak, this assumption requires further scrutiny. In fact, examination of figure 25 below provides evidence that the microwave sensor in No Filter mode performs better as a measure of water level variance in the presence of waves than the microwave sensor in Fast Change mode. Therefore, the assumption of the Aquatrak as a preferred reference is questionable. Finally, as water level energy increases there is the emergence of an asymmetric tail at negative range to water levels. This is consistent with the emergence of wave-like statistics (Rayleigh) from non-wave (Gaussian) distributions.

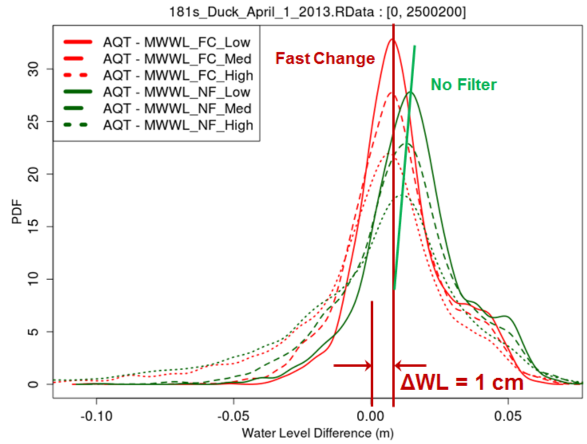

Fig. 22. Probability density functions of range to water level difference (acoustic - microwave) for April 2013 at Duck. Density functions are shown for low ($0 < \sigma < 1/3$) medium ($1/3 < \sigma < 2/3$) and high ($\sigma > 2/3$) partitions of the data.

Figure 23 plots PSD estimates for water level data during a period of low surface variance (April 9 - 11, 2013) for the Aquatrak and microwave sensors operating in both Fast Change and No Filter modes. These responses are consistent with other data revealing good coherence between the acoustic and microwave sensors in the wind wave band, lower variance of the microwave sensor in Fast Change mode, roll-off of the acoustic system at short periods and evidence of the protective well resonance.

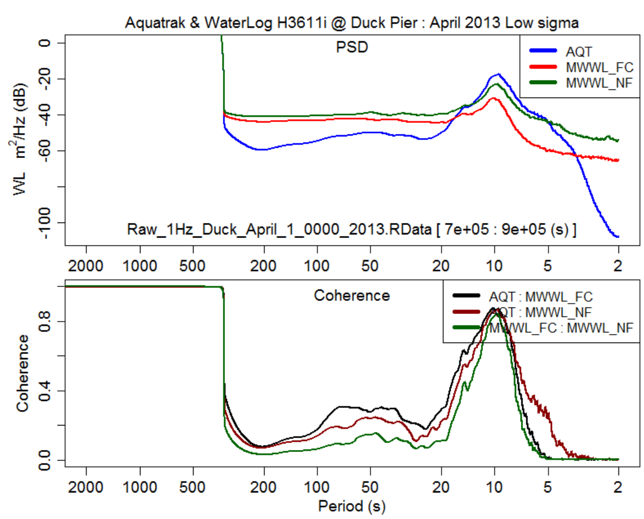

Fig. 23. PSD and coherence of acoustic and microwave water level data at Duck NC for April 9 - 11, 2013, a period of low surface energy.

PSD estimates for all three water level sensors covering April 1 - 28, 2013 are shown in figure 24. Spectral response is consistent with other observations.

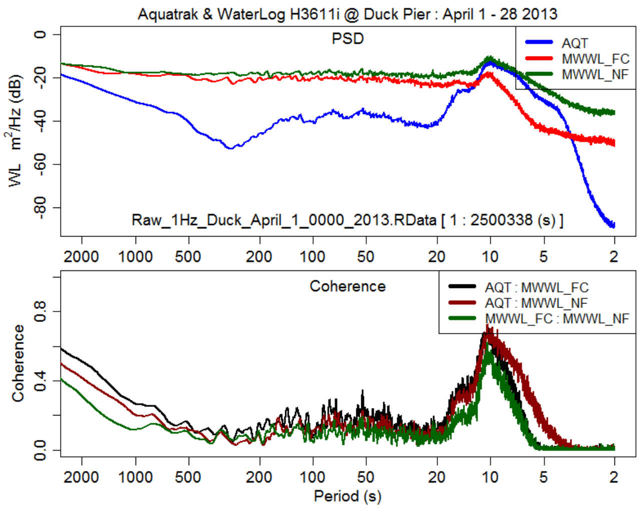

Fig. 24. PSD and coherence of acoustic and microwave water level data at Duck NC for April 2013.

As shown in *Standard Deviation and Significant Wave Height*, there is a robust relationship between water level σ and significant wave height. Figure 25 presents linear regression results for Hm_0/σ for all three sensors in April 2013. Consistent with previous results, the microwave sensor more closely matches the canonical definition of wave-driven water level variance. It is interesting to note that No Filter mode performs best. This may be an indication that presumptive veracity of the Aquatrak system representing water level variance is misleading (see figure 22).

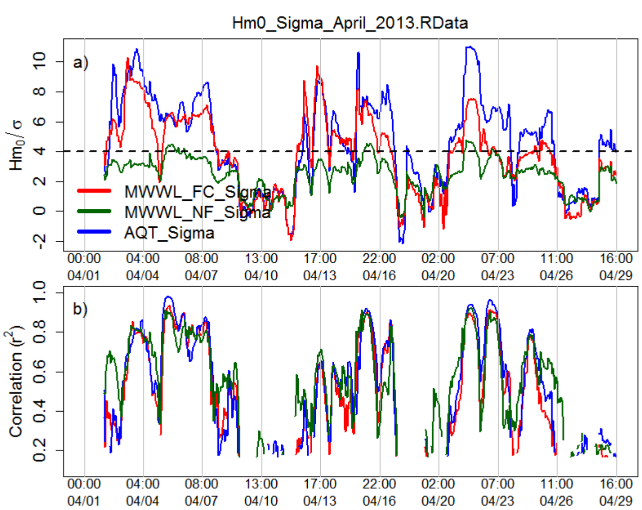

Fig. 25. Linear regression of DQAP σ and significant wave height for the acoustic and microwave sensors during April 2013. a) Fit coefficients b) Correlation coefficient. Values are shown only if the p-value exceeded the 95% confidence interval. The dashed line shows the canonical definition of $\mathrm{Hm}_0 = 4\sigma$.

Water level differences, estimated draw-down and significant wave height for October 2013 is shown in figure 26. Negative water level differences are captured by the draw-down model, and one should take note of the magnitude of water level differences (15 cm) during the large wave event on April 9.

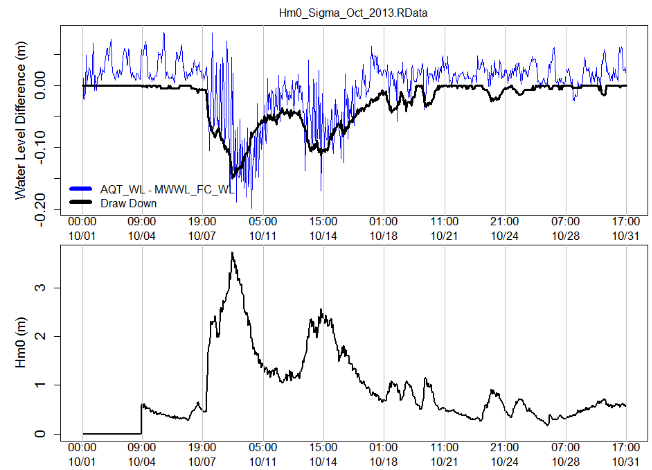

Fig. 26. Hourly data and draw-down corrections from Duck North Carolina in April 2013. a) Water level difference between the acoustic and microwave sensors (blue) and protective well draw-down estimates (black). b) Significant wave height.

La Jolla

The La Jolla tide gauge is located on the Scripps Oceanographic Institute research pier. The Aquatrak system is located on the south side of the pier receiving direct sunlight to the protective well throughout the year. The protective well is one of the longest in use, and these two features result in significant Aquatrak temperature errors. The Phase II test plan did not install a wave gauge but relies upon the Coastal Data Information Program (CDIP) wave gauge at the pier. Figure 27 show the CDIP wave height and period at Scripps Pier for October 2013, indicating small to medium wave events on October 10^{th} and 28^{th}, and small waves from the 2^{nd} through the 4^{th}.

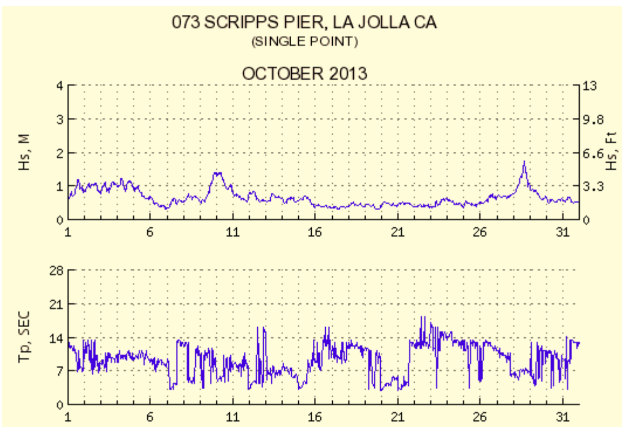

Fig. 27. CDIP significant wave height and period at Scripps Pier.

A power spectral density estimate of the microwave sensor data over the month of October is shown in figure 28. This might be considered a prototypical spectra for ocean waves with dominant energy in the wind-wave band. (Although the peak near 110 second periods is not representative of open ocean spectra, and likely represent infragravity waves generated by shelf interactions with wind-wave forcing.)

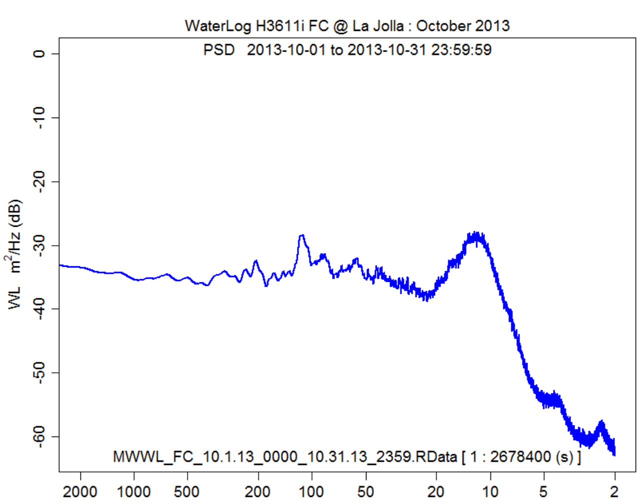

Fig. 28. PSD estimate of microwave water level for October 2013 at La Jolla.

Figure 29 plots water level differences with the acoustic temperature corrections and wave draw-down estimates. It is somewhat difficult to see, but inspection reveals that the temperature and draw-down errors account for the bulk of the water level differences.

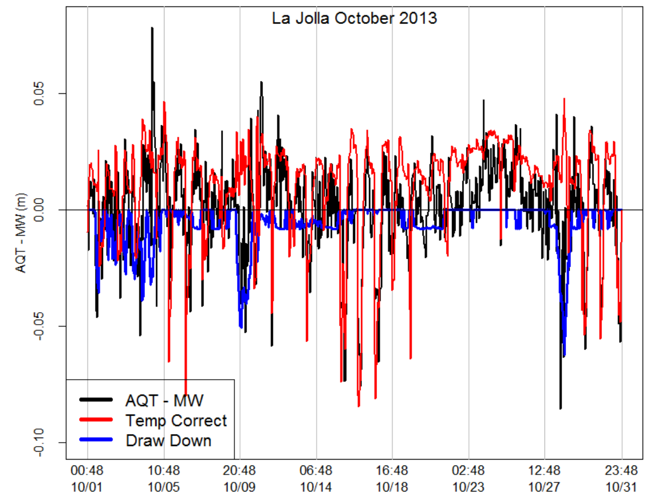

Fig. 29. Sensor water level difference (acoustic - microwave), acoustic temperature corrections and wave-induced draw-down at La Jolla for October 2013.

To better assess the water level differences and corrections for October 2013, figure 30 separately plots the sensor water level differences (top) and the combined temperature and draw-down corrections (bottom). Even a casual observation suggests a high degree of correspondence, and a linear regression of the two finds a correlation coefficient of 0.74 with r^2 of 0.47.

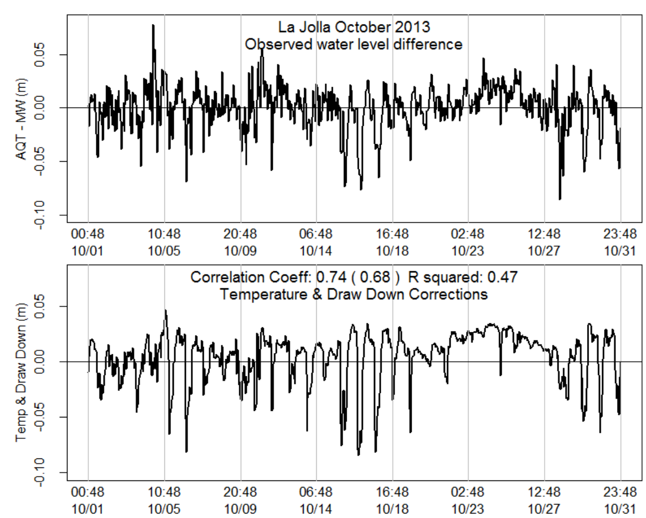

Fig. 30. Observed water level difference (top) and combined temperature and draw-down corrections (bottom) at La Jolla for October 2013.

Lake Worth

Lake Worth is an intermediate wave environment, but does experience large wave events from both Northeasters and Hurricanes. Data at Lake Worth are available from September through November 2013. Figure 31 plots PSD estimates for the acoustic and microwave sensor for September 2013. The large spectral distortion of the acoustic sensor at a period of 5 seconds is incoherent with the microwave observations, and provides compelling evidence that resonance of the protective well is contributing to the distortion.

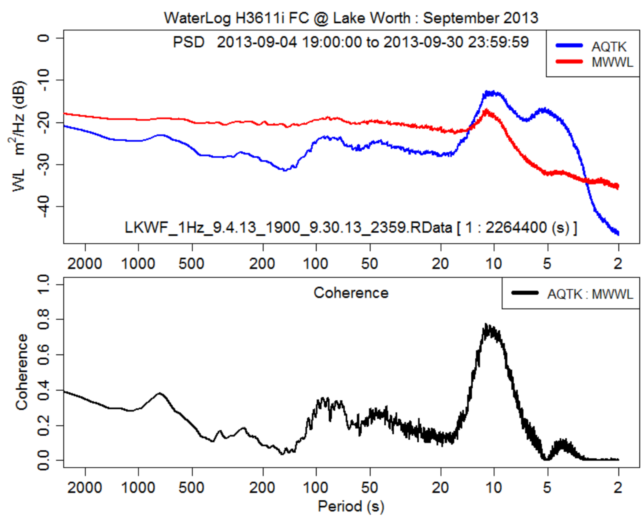

Fig. 31. PSD and coherence of acoustic and microwave water level data at Lake Worth for September 2013.

Figure 32 shows a comparison of significant wave height with microwave standard deviation in the upper panel and the sensor water level differences with acoustic temperature and wave draw-down corrections in the lower panel. Lake Worth resides in a subtropical climate and acoustic temperature corrections are not normally applied. However, figure 32 shows that temperature errors of 2 - 4 cm are common. Waves were generally small (less than 1 m) for the month, however wave events of 1 m height did occur on the 16th and 28th with the draw-down model correctly attributing the observed draw-down. The wave event on the 19th was smaller, but still produced a noticeable draw-down. Given the extreme distortions of spectral energy at 5 seconds, it is likely that resonance of the protective well contributes to deviation from the modeled draw-down.

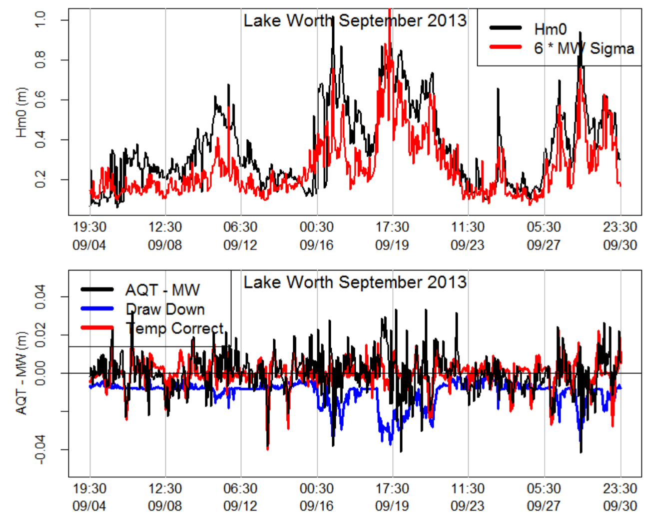

Fig. 32. Significant wave height and microwave DQAP standard deviation (top) at Lake Worth in September 2013. Water level difference (acoustic - microwave) with acoustic temperature and wave draw-down corrections (bottom).

Figure 33 presents PSD estimates for the acoustic and microwave sensor for October 2013. The extreme spectral distortion of the acoustic sensor from 4 to 8 seconds is incoherent with the microwave observations indicating that resonance of the protective well is contributing this distortion.

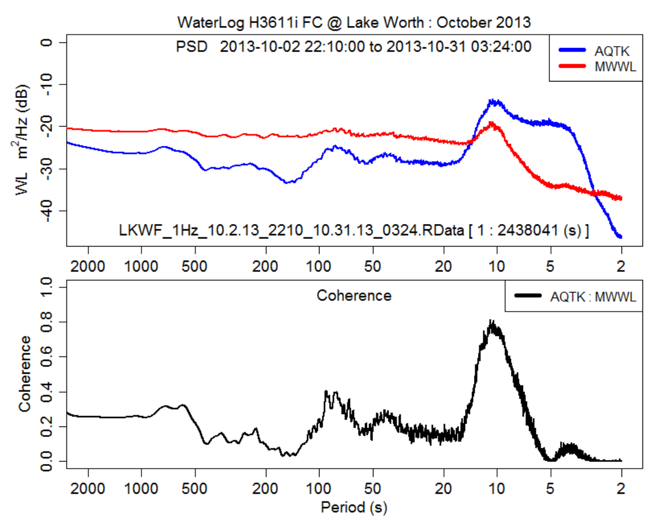

Fig. 33. PSD and coherence of acoustic and microwave water level data at Lake Worth for October 2013.

A comparison of significant wave height with microwave standard deviation, and water level differences with acoustic temperature and wave draw-down corrections for October is shown in figure 34. Temperature errors of 2 - 4 cm are common. Waves were generally small during October, less than 0.6 m, and the draw-down model over-predicts draw-down during the three small wave events. This can be addressed with adjustment of the minimum wave threshold to the draw-down model. The wave event on the 30th is accurately captured by the draw-down model.

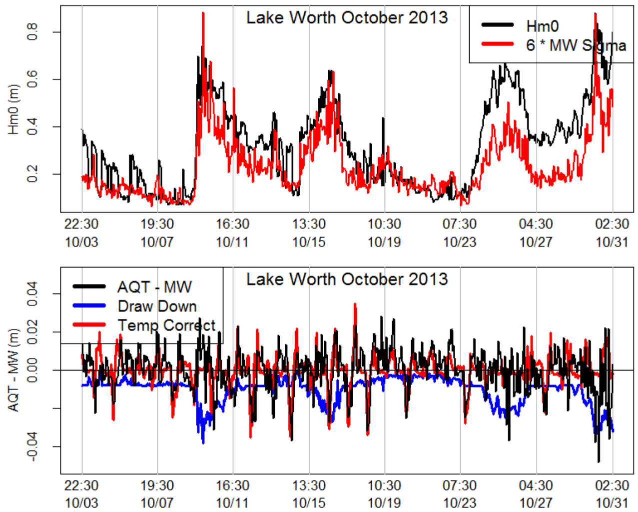

Fig. 34. Significant wave height and microwave DQAP standard deviation (top) at Lake Worth in October 2013. Water level difference (acoustic - microwave) with acoustic temperature and wave draw-down corrections (bottom).

PSD and coherence estimates for the acoustic and microwave sensor for November 2013 are shown in figure 35. At this point, a consistent picture of spectral distortion from the protective well resonance is clear.

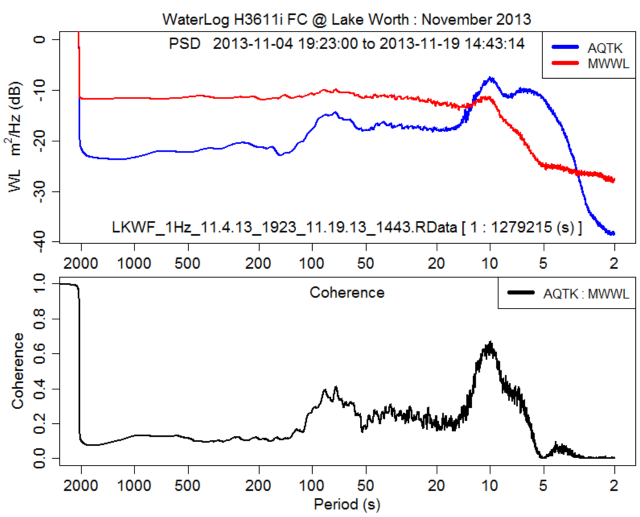

Fig. 35. PSD and coherence of acoustic and microwave water level data at Lake Worth for November 2013.

Figure 36 plots comparison of significant wave height with microwave standard deviation in the upper panel and sensor water level differences with acoustic temperature and wave draw-down corrections in the lower panel. There were three wave events in November that exceeded 1 m significant wave height, and during each wave event the draw-down model captures the observed water level differences. Oscillation of water levels from the protective well resonance is thought to account for the observed pile ups during wave events. Temperature corrections are essentially absent during the month.

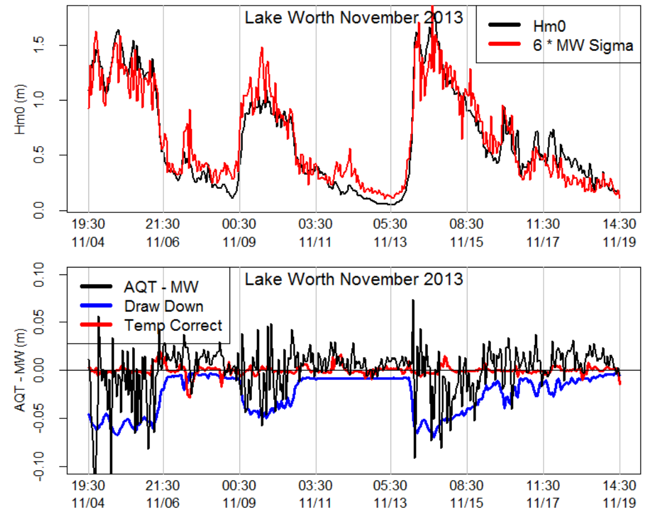

Fig. 36. Significant wave height and microwave DQAP standard deviation (top) at Lake Worth in November 2013. Water level difference (acoustic - microwave) with acoustic temperature and wave draw-down corrections (bottom).

Monterey

Monterey was selected as an intermediate wave environment, although breaking waves at the sensor site are rare due to the semi-enclosed nature of Monterey Harbour and wharf inside the breakwater. Based on analysis of data covering the period September 14 - November 29, 2013, the following conclusions are supported:

1. Water level differences suggest that temperature issues associated with the Aquatrak sound speed dependence are not a primary error source at Monterey.
2. Water level differences between the acoustic and microwave sensors exhibit a tidally-locked component 90° out of phase with water level amplitude. Flood tide produces a negative difference (microwave level higher than acoustic level) while ebb tide presents a positive water level difference (acoustic higher than microwave). Since the acoustic sensor is closer to shore, it is suggested that this component represents the mean surface slope.
3. Wave induced draw-down in the Aquatrak is not a primary error source for wave heights less than 0.5 m.
4. There is good correlation between microwave DQAP standard deviation and significant wave height (Hm_0).
5. Spectral analysis presents a robust and persistent set of water level resonant modes (seiche). Dominant components are seen at periods near 36, 27 and 2 minutes with amplitudes in the range of 0.45 m. The longer period modes represent bay-wide resonances, while the 2 minute mode likely represents a resonance within Monterey Harbour. Other notable resonances are found at periods of 22, 19, 16, 11, 9 and 4 minutes. This harmonic structure is consistent with measurements and models of resonance in Monterey Bay [29, 30]. Water level amplitudes of individual modes range from 30 to 475 cm, therefore, if several modes were to synchronize constructively water level variations well in excess of 1 m are plausible.

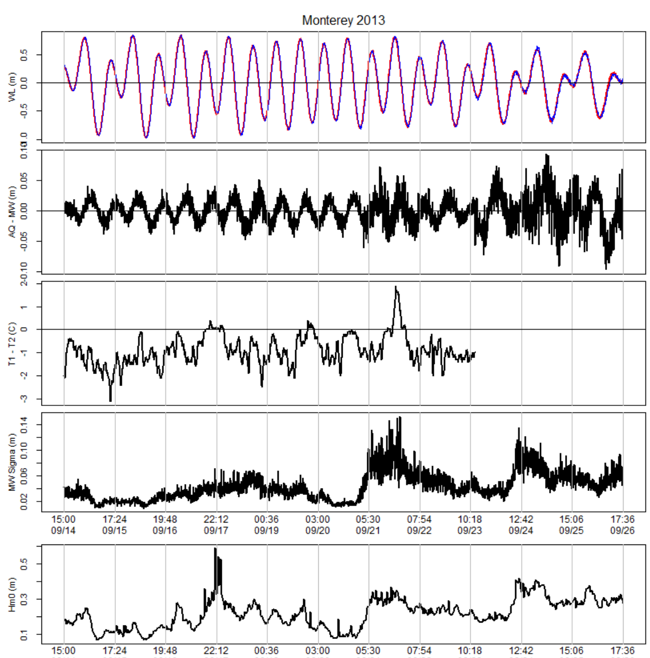

Fig. 37. Monterey data for September 14 - 26, 2013. WL is the demeaned DQAP water level, microwave data are red, acoustic data are blue. AQ - MW is the water level difference. T1 - T2 is the temperature difference of the two thermistors. MW Sigma is the DQAP standard deviation (σ) of the microwave data. Hm0 is the significant wave height.

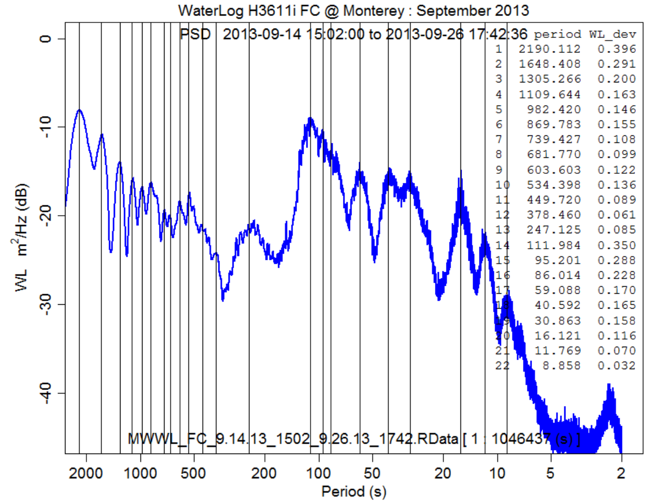

Fig. 38. PSD estimate of microwave water level at Monterey for September 14 - 26, 2013. Vertical lines mark frequencies of interest. The inset table lists the period of oscillation in seconds for each vertical line and the corresponding water level oscillation amplitude in meters.

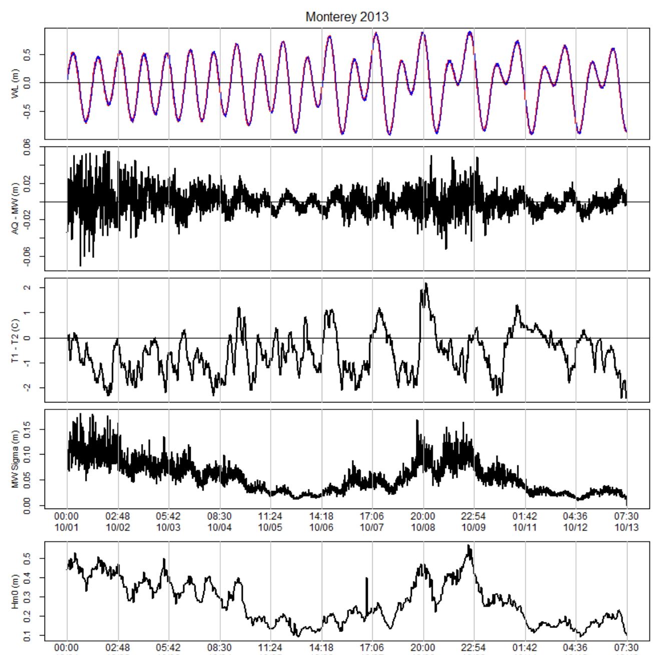

Fig. 39. Monterey data for October 1 - 13, 2013. WL is the demeaned DQAP water level, microwave data are red, acoustic data are blue. AQ - MW is the water level difference. T1 - T2 is the temperature difference of the two thermistors. MW Sigma is the DQAP standard deviation (σ) of the microwave data. Hm0 is the significant wave height.

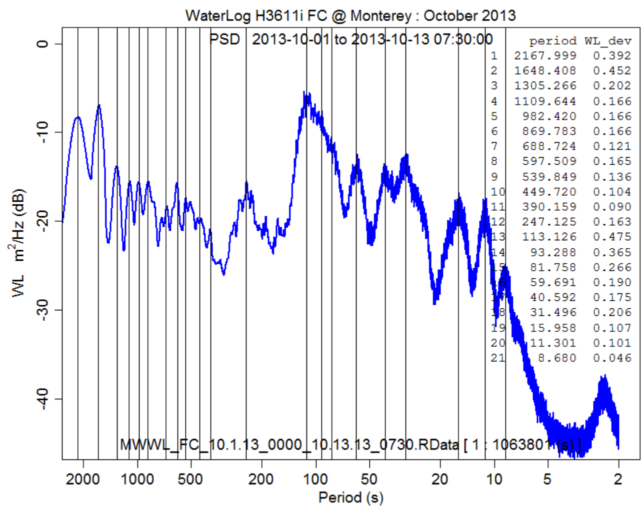

Fig. 40. PSD estimate of microwave water level at Monterey for October 1 - 13, 2013. Vertical lines mark frequencies of interest. The inset table lists the period of oscillation in seconds for each vertical line and the corresponding water level oscillation amplitude in meters.

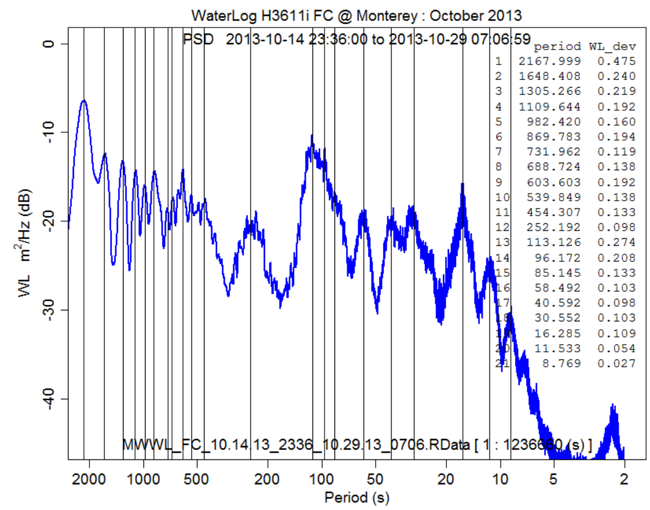

Fig. 42. PSD estimate of microwave water level at Monterey for October 14 - 29, 2013. Vertical lines mark frequencies of interest. The inset table lists the period of oscillation in seconds for each vertical line and the corresponding water level oscillation amplitude in meters.

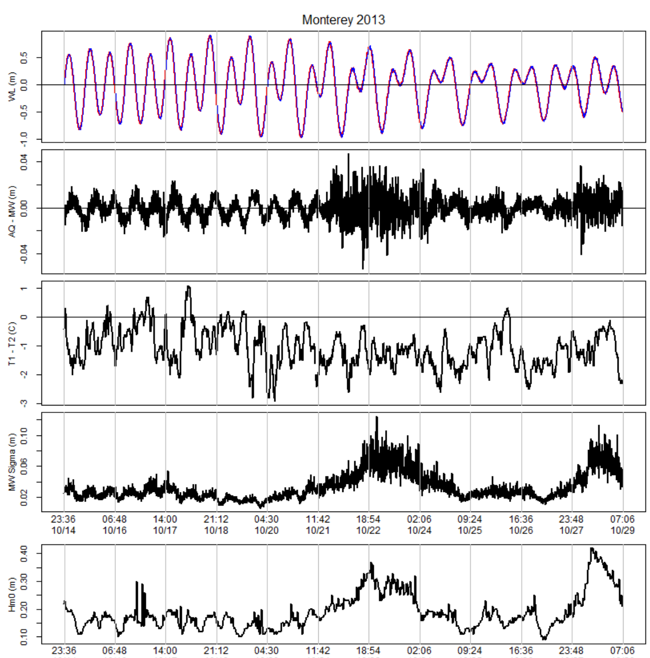

Fig. 41. Monterey data for October 14 - 29, 2013. WL is the demeaned DQAP water level, microwave data are red, acoustic data are blue. AQ - MW is the water level difference. T1 - T2 is the temperature difference of the two thermistors. MW Sigma is the DQAP standard deviation (σ) of the microwave data. Hm0 is the significant wave height.

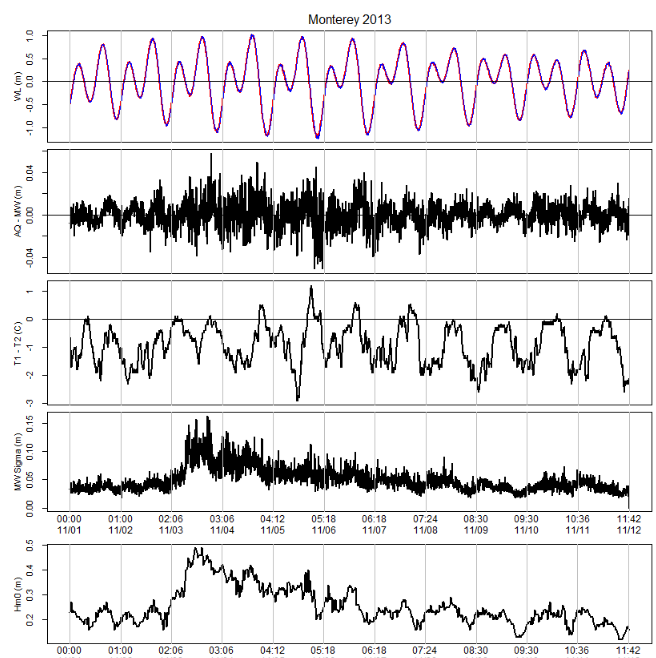

Fig. 43. Monterey data for November 1 - 12, 2013. WL is the demeaned DQAP water level, microwave data are red, acoustic data are blue. AQ - MW is the water level difference. T1 - T2 is the temperature difference of the two thermistors. MW Sigma is the DQAP standard deviation (σ) of the microwave data. Hm0 is the significant wave height.

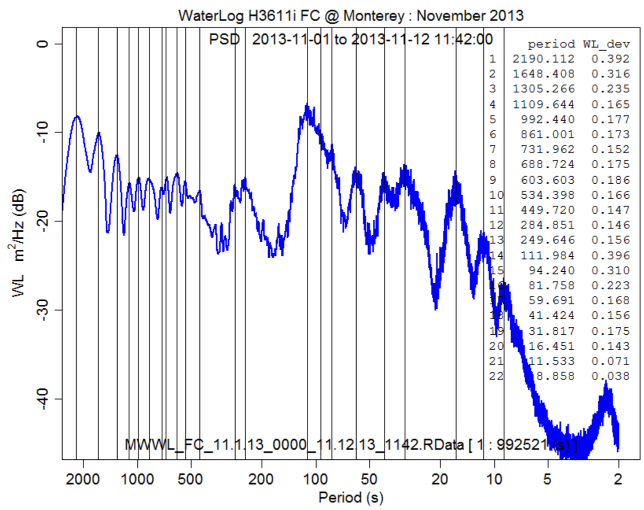

Fig. 44. PSD estimate of microwave water level at Monterey for November 1 - 12, 2013. Vertical lines mark frequencies of interest. The inset table lists the period of oscillation in seconds for each vertical line and the corresponding water level oscillation amplitude in meters.

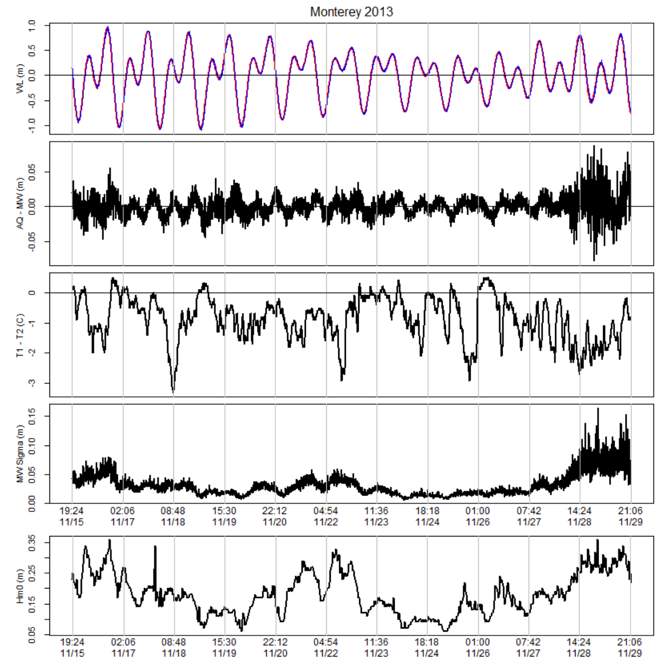

Fig. 45. Monterey data for November 15 - 29, 2013. WL is the demeaned DQAP water level, microwave data are red, acoustic data are blue. AQ - MW is the water level difference. T1 - T2 is the temperature difference of the two thermistors. MW Sigma is the DQAP standard deviation (σ) of the microwave data. Hm0 is the significant wave height.

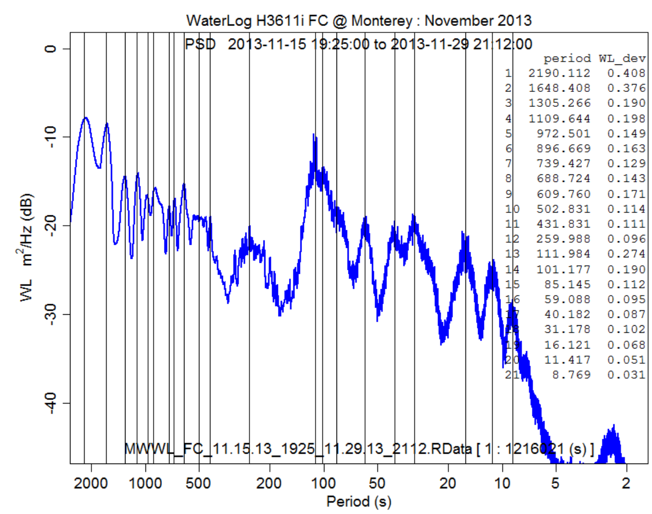

Fig. 46. PSD estimate of microwave water level at Monterey for November 15 - 29, 2013. Vertical lines mark frequencies of interest. The inset table lists the period of oscillation in seconds for each vertical line and the corresponding water level oscillation amplitude in meters.

1. Integrated Ocean Observing System, NOAA http://www.ioos.noaa.gov/ (2013).
2. Joint Technical Commission for Oceanography and Marine Meteorology (JCOMM) of the World Meteorological Organisation and the Intergovernmental Oceanographic Commission. The Global Sea Level Observing System. http://www.gloss-sealevel.org/ (2013).
3. Edwing R., Next Generation Water Level Measurement System NGWLMS Site Design, Preparation, and Installation Manual. http://tidesandcurrents.noaa.gov/publications/NextGenerationWaterLevelMeasurementSystemMANUAL.pdf (1991).
4. Porter D. L. and Shih H. H., Investigation of Temperature Effects on NOAAs Next Generation Water Level Measurement System. Journal of Atmospheric and Oceanic Technology, Vol. 13, pg. 714–725 (1996).
5. Hunter J. R., On the Temperature Correction of the Aquatrak Acoustic Tide Gauge. Journal of Atmospheric and Oceanic Technology, Vol. 20, pg. 1230–1235 (2003).
6. Shih H. H. and Rogers D., Error analysis for tide measurement systems utilizing stilling wells. NOAA Tech. Rep., U.S. Department of Commerce, NOAA, Office of Ocean Technology and Engineering Services (1981).
7. Boon J. and Heitsenrether R., Multi-sensor evaluation of microwave water level error. Proc. Oceans 12, October 14-19, Hampton Roads, VA (2012).
8. Morris C. S. and DiNardo S. J. and Christensen E. J., Overview of the TOPEX/Poseidon Platform Harvest verification experiment. Marine Geodesy, Vol. 18, pg. 25–37 (1995).
9. Parke M. E. and Gill S. K., On the sea state dependence of sea level measurements at platform Harvest. Marine Geodesy, Vol. 18, pg. 105–111 (1995).
10. Integrated Ocean Observing System, A National Operational Wave Observation Plan. Integrated Ocean Observing System (IOOS) plan for a surface-wave monitoring network for the United States http://www.ioos.noaa.gov/library/wave_plan_final_03122009.pdf (2009).
11. Heitsenrether R., Using Microwave Range Sensors for Long Term Remote Sensing of Ocean Surface Dynamics. AMS 17th Conference on Atmospheric and Oceanic Fluid Dynamics, June 8-12, Stowe, VT, https://ams.confex.com/ams/17Fluid15Middle/webprogram/Paper154150.html (2009).
12. Heitsenrether R., Understanding the impact of surface waves on Microwave Water Level measurements. Proc. Oceans 08, September 15-18, Quebec City, QC (2008).
13. Boon J., Heitsenrether R. and Bushnell M., Microwave-acoustic water level sensor comparisons: sensor response to change in oceanographic and meteorological parameters. Proc. Oceans 09, October 26-29, Biloxi, MS (2009).
14. Park J. and Heitsenrether R., Microwave Water Level Transition to Operations (MWWL TOP) WaterLog H-3611 Test Plan Part II: Sensor Response to Dynamic Water Levels, January 24 2013, NOAA Center for Operational Products and Services http://intranet.nos-tcn.noaa.gov/media/wikidocs/ED/DET/MWWL/WaterLogCharacterizationTestPlan_Part_II_v0.3.pdf, (2013).
15. Park J., Heitsenrether R., et al., Microwave Water Level Transition to Operations (MWWL TOP) Part II Field Test: Sensor Response to Dynamic Water Levels Installation Plan, NOAA Center for Operational Products and Services, August 29 2013. http://intranet.nos-tcn.noaa.gov/media/wikidocs/ED/DET/MWWL/MWWLPartIIFieldTest_InstallationPlan_v5.pdf (2013).
16. Hensley W., Test System Install: OSTEP and DET Return of the Jedi, USACE FRF Duck NC, NOAA Center for Operational Products and Services, May 2013. http://intranet.nos-tcn.noaa.gov/media/wikidocs/OSTEP/Trip\%20Reports/2013_01_15_OSTEP_DET_TripReport.pdf (2013).
17. Park J. et al., MWWL Phase II Installation: La Jolla and Monterey CA. NOAA Center for Operational Products and Services, October 28, 2013. http://intranet.nos-tcn.noaa.gov/media/wikidocs/ED/DET/MWWL/MWWL_PhaseII_Installation_LaJolla_Monterey_v0.2.pdf (2013).
18. Heitsenrether R., Installation of a Microwave Radar Water Level Sensor Test Platform at Lake Worth, FL NWLON station. NOAA Center for Operational Products and Services, September 2, 2013. http://intranet.nos-tcn.noaa.gov/media/wikidocs/OSTEP/201308_LakeWorthMWWLInstallTripReport_final.pdf (2013)
19. Shih H. H., The Water Level Response Inside an Open Protective Well to Surface Wave Excitation. NOAA Tech. Rep., U.S. Department of Commerce, NOAA, Office of Ocean Technology and Engineering Services, September (1981).
20. Serway R. A. and Jewett J. A., Physics for Scientists and Engineers. Brooks/Cole. Ed. 9, pg. 468–471 (2008).
21. Heitsenrether R. M. and Davis E., Limited Acceptance of the Design Analysis WaterLog H-3611i Microwave Radar Water Level Sensor. U.S. Department of Commerce, NOAA Technical Report NOS CO-OPS 061, March 2011. http://tidesandcurrents.noaa.gov/publications/Technical_Report_NOS_CO-OPS_061.pdf (2011).
22. NOAA, Environmental Measurement Systems Sensor Specifications and Measurement Algorithm. http://tidesandcurrents.noaa.gov/publications/CO-OPS_Measure_Spec_07_July_2013.pdf (2013).
23. Munk W. H., Origin and generation of waves. Proc. 1st International Conference on Coastal Engineering, ASCE, Long Beach, CA, pg. 1–4 (1950).
24. Vogt C. J.,Croucher A. and Mooney J., The Aquatrak Water Level Sensor Field Test at Shady Side, Maryland. The Johns Hopkins University Applied Physics Laboratory, STD-N-494, Submarine Technology Department, December (1986).
25. Park J., and Shabbir A., Temperature Gradient Effect on the Sound Path Measurement of Aquatrak Acoustic Tide Gauge, NOAA Center for Operational Products and Services. http://intranet.nos-tcn.noaa.gov/media/wikidocs/ED/DET/Aquatrak/AquatrakTemperatureProfiles_Shabbir_2013.pdf (2013).
26. Park J., and Heitsenrether R., WaterLog H-3611i Test Results Part I: Sensor Characterization, NOAA Center for Operational Products and Services. http://intranet.nos-tcn.noaa.gov/media/wikidocs/ED/DET/MWWL/WaterLog_Phase_I_TestResults_v0.11.pdf (2013).
27. NOAA, Duck, NC Station ID: 8651370 http://tidesandcurrents.noaa.gov/stationhome.html?id=8651370 (2013).
28. NOAA, Meteorological Observations, Duck NC, Station ID: 8651370, {http://tidesandcurrents.noaa.gov/data_menu.shtml?bdate=20120427\&edate=20120428\&metinterval=\&unit=1\&shift=g\&stn=8651370+Duck\%2C+NC\&type=Meteorological+Observations\&format=View+Plot} (2012).
29. Wilson B.W., Hendrickson J.A. and Kilmer R.E., Feasibility study for a surge-action model of Monterey Harbor, California. U.S. Army Engineer Waterways Experiment Station, Corps of Engineers, Vicksburg, MS, Contract Report No. 2-136, http://www.dtic.mil/dtic/tr/fulltext/u2/684953.pdf, (1965).
30. Breaker L.C., Murty T.S., Norton J.R., Carroll D., Comparing sea level response at Monterey, California from the 1989 Loma Prieta Earthquake and the 1964 Great Alaskan Earthquake, Science of Tsunami Hazards, Vol. 28, No. 5, page 255 (2009).
31. Kruger J., and Dunning D., Unskilled and unaware of it: How difficulties in recognizing one's own incompetence lead to inflated self-assessments. Journal of Personality and Social Psychology, Vol 77(6), pg. 1121-1134 http://psycnet.apa.org/journals/psp/77/6/1121/ (1999).